Humidity Impact on Kitchen Fronts

Erik Persson and Philip Ward

DIVISION OF INNOVATION | DEPARTMENT OF DESIGN SCIENCES
FACULTY OF ENGINEERING LTH | LUND UNIVERSITY
2024

MASTER THESIS

Humidity Impact on Kitchen Fronts

Erik Persson and Philip Ward

LUND
UNIVERSITY

Humidity Impact on Kitchen Fronts

Published by
Department of Design Sciences
Faculty of Engineering LTH, Lund University
P.O. Box 118, SE-221 00 Lund, Sweden

Publicerad av
Institutionen för designvetenskaper
Lunds Tekniska Högskola, Lunds universitet
Box 118, 221 00 Lund

Subject: Product Development (MMKM05)
Division: Innovation
Supervisor: Joze Tavcar
Examiner: Elin Olander

Ämne: Produktutveckling (MMKM05)
Avdelning: Innovation
Huvudhandledare: Joze Tavcar
Examinator: Elin Olander

Abstract

Durable and robust product development is crucial for fulfilling customer expectations and ensuring satisfaction. In this context, thorough testing plays an essential role in identifying and addressing potential defects before products reach the final customer. IKEA, with its worldwide presence, aims to enhance its understanding of humidity's impact on kitchen fronts, one of the main product areas. Given the diverse climatic conditions across IKEA's markets, it is essential to ensure that products can withstand stresses derived from variations in temperature and humidity. The durability and quality of the kitchen fronts should thus be independent of the customer's geographical location.

This study looks into the relationship between temperature, humidity, and its impact on kitchen fronts, exploring the possibility of accelerating testing while maintaining realistic results. Through experimentation and analysis, it was discovered that relative humidity predominantly influences water sorption over time, while temperature determines the sorption rate. These findings align with the theoretical framework, indicating that equilibrium moisture content is mainly determined by relative humidity, while temperature influences the water vapor permeability and, consequently, the rate of water vapor into the fronts.

In summary, this study highlights the relationship between humidity and temperature, and their impact on the kitchen front. Thus, providing valuable insights that can serve as a foundation for durable product development and the implementation of effective test parameters.

Keywords: Medium Density Fiberboard; Relative Humidity; Temperature; Design of Experiments; Accelerated Testing

Sammanfattning

Hållbar och robust produktutveckling är avgörande för att tillgodose kundernas förväntningar och säkerställa kundnöjdhet. I denna kontext spelar noggrann testning en väsentlig roll för att identifiera och åtgärda potentiella defekter innan produkterna når slutkonsumenten. IKEA, med sin globala närvaro, strävar efter att utöka sin kunskap om luftfuktighetens inverkan på köksfronter, vilket är ett av de viktigaste produktområdena. Med tanke på klimatvariationerna på IKEAs marknader är det avgörande att säkerställa att produkterna kan motstå de påfrestningar som skapas av variationer i temperatur och luftfuktighet. Köksfronternas hållbarhet och kvalitet ska således vara oberoende av slutkonsumentens geografiska position.

Denna studie undersöker sambandet mellan luftfuktighet, temperatur och deras inverkan på köksfronter, samt möjligheten att accelerera testningen och samtidigt upprätthålla realistiska resultat. Genom tester och analyser upptäcktes att relativ luftfuktighet främst påverkar vattenabsorptionen över tid, medan temperaturen bestämmer hastigheten på absorptionen. Dessa resultat överensstämmer med det teoretiska ramverket och indikerar att luckornas mättnadshalt främst bestäms av relativ luftfuktighet, medan temperaturen påverkar permeabiliteten och därmed hastigheten på vattenångan som tränger in i luckorna.

Sammanfattningsvis betonar detta projekt sambandet mellan luftfuktighet och temperatur samt deras inverkan på köksfronterna, vilket kan utgöra en grund för hållbar produktutveckling och implementeringen av effektiva testparametrar.

Nyckelord: Medium Density Fiberboard; Relativ Fuktighet; Temperatur; Experimentell Design; Accelererad Testning

Acknowledgments

First and foremost, we would like to thank everyone at IKEA who helped us throughout this project. This includes our supervisor at IKEA, Karin Jenskog, who has always been available, answered all our questions, and guided us along the way. We are also grateful to Rasmus Hyllengren and Martin Strand for helping us narrow the scope of the project during its initial phase. Jan-Olof Fechter provided valuable expertise in MDF, engaging us in several interesting discussions. Finally, a big thank you to Magdalena Söderström and Sven-Ingvar Johansson at the IKEA Test Lab for their assistance during the test phase. Without you all, this project would not have been possible.

We would also like to express our gratitude to our supervisor at LTH, Jože Tavčar, for his continuous support and help throughout the project. Additionally, we extend our thanks to Maria Fredriksson and Jonas Niklewski at the Division of Building Material and Structural Engineering for their expertise on the impact of moisture on wood.

Lund, May 2024

Erik Persson and Philip Ward

Contents

List of Figures

List of Tables

Nomenclatur

E_a	Activation energy	J
γ_0	Pre-exponential factor	-
M_a	Molar mass of air	kg/mol
M_w	Molar mass of water	$kg \cdot mol^{-1}$
N_a	Number of air moles	-
N_w	Number of water moles	-
P_{sat}	Saturated vapor pressure	Pa
P_w	Partial vapor pressure	Pa
R	Reaction rate	$M \cdot s^{-1}$
Z	Transmission resistance	s/m
δ_v	Water vapor permeability	m^2/s
g	Moisture diffusion	$kg/(m^2 \cdot s)$
k	Boltzmann's constant	$J \cdot K^{-1}$
m_a	Mass dry air	kg
m_w	Mass water vapor	kg
ω	Humidity ratio	kg/kg
ω_e	Moisture content	%
φ	Relative humidity	%
ξ	Moisture capacity	kg/m^3
v	Vapor capacity	kg/m^3
v_s	Saturated vapor content	kg/m^3
ζ	Total measurement error	-

Chapter 1

Introduction

Durable and robust design is essential in product development, to fulfill customers' expectations. Thus, all products must continuously undergo various tests to identify and address any defects or flaws before the product reaches the customer. By conducting this proactive approach, quality concerns can be kept at a low level, while customer satisfaction and trust will remain high.

IKEA is aiming to enhance its understanding of humidity and its influence on one of its major product areas, kitchen fronts. Due to the global presence of IKEA products, it is essential that these products can withstand the diverse climatic stresses present in various regions worldwide. Given the variations in humidity across IKEA's global markets and in response to customers' expectations regarding the durability of the product, precise requirements and testing methods that accurately mirror real-life conditions in different households are crucial.

1.1 Background

In the small village of Älmhult, located in the woods of Småland, Sweden, IKEA was founded in 1943 by Ingvar Kamprad. At the age of 17, Kamprad began his journey by selling various products, such as pens, through efficient distribution. Fast forward to today, IKEA has grown to become one of the most recognizable companies in the world with a

vision to "*create a better everyday life for the many people*" [11, 12].

Today, IKEA has a worldwide presence, with over 450 stores in 63 different markets [13]. Thus, the durability and quality of the kitchen fronts should be independent of the customer's geographical location. A classification of various climate regions seen globally is presented in Figure 1.1, where the most extreme areas, in terms of relative humidity and temperature, are highlighted with red dots. These regions represent the worst-case scenarios for environmental stress on kitchen fronts. [1]

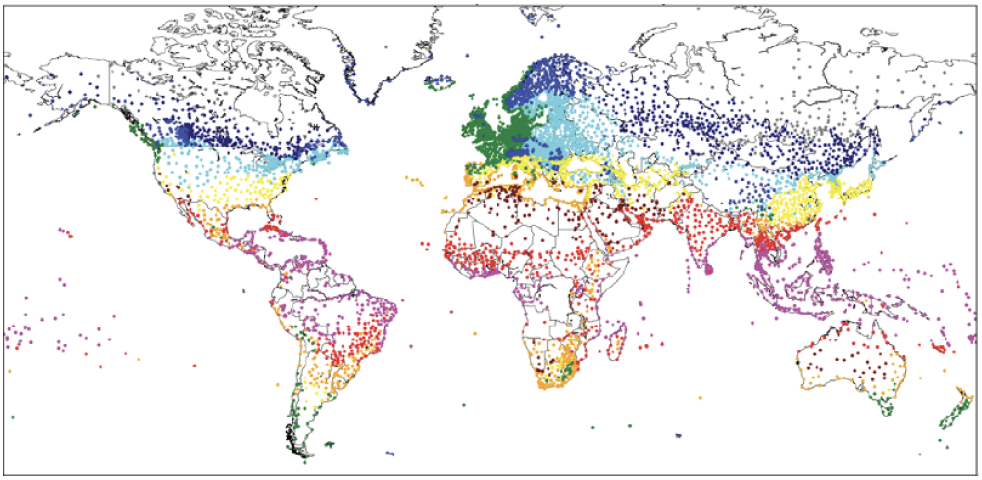

Figure 1.1: Classifications temperature and humidity [1]

IKEA has a warranty of 25 years on their kitchen fronts [14]. However, maintaining this warranty will require high-quality kitchen fronts, which may be challenging due to varying humidity levels in different locations. Figure 1.2 shows two graphs of measured indoor temperature and relative humidity over six months in Shenzhen, China, a city within one of the extreme regions marked in red in Figure 1.1. These graphs offer insight into the climatic fluctuations that kitchen fronts in these regions are subjected to over time. [1]

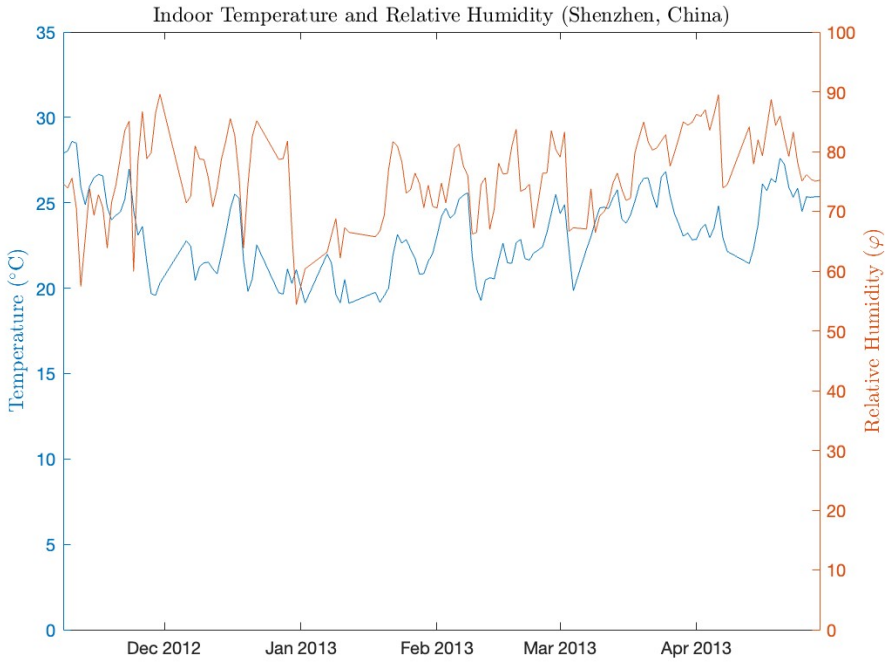

Figure 1.2: Indoor temperature in Shenzhen, China [1]

Another city that faces extreme climatic conditions is Mumbai, India. Over a five-month investigation, IKEA found that on a quarter of the days, humidity levels spiked above 80 %. Additionally, around 6 % of the days registered an average hourly peak surpassing 90 % relative humidity. When looking at daily averages, it was noted that approximately 12 % of the days exceeded 80 % humidity, with a smaller yet notable portion reaching over 85 %. This clearly shows the challenging conditions IKEA's kitchen fronts must endure in Mumbai. [1]

The climate conditions during transport and storage are another important concern for IKEA. Based on measurements and research, temperatures of up to 60°C and relative humidity levels ranging from 70 % to 95 % have been recorded in containers. However, these conditions do not occur simultaneously, as higher relative humidity levels are associated with rapid temperature drops. In one of IKEA's distribution centers in Shanghai, long-term relative humidity was found to be around 75-85 %

and the temperature was 22-34 °C. There have also been measurements at counting points which are around 95 % relative humidity. [1]

1.2 Problematization

Developing and evaluating test methods that mirror real-life conditions can be a difficult and complex process. Stresses caused by mechanical loads, such as opening and closing drawers, are easy to simulate in a test environment since these loads are easy to quantify and failures are easily identified. However, defects on kitchen fronts that can be derived from high humidity levels are harder to quantify and determine, since the defect is identified by visual inspection and thus introduces another complexity with the subjectivity related to the inspector.

Accelerated testing in a humidity chamber can be used to simulate a product's durability and detect potential flaws or failures induced by humidity. This is achieved by either maintaining a constant relative humidity and temperature, see Section 2.6, or subjecting the product to cyclic stress through variations in temperature and relative humidity within the chamber. However, this process is time-consuming, making it desirable to shorten the testing period while still ensuring realistic results.

1.3 Aim and Objective

This thesis aims to investigate the impact of variations in temperature and humidity on kitchen fronts, focusing on the most extreme conditions identified globally. By analyzing different levels of these factors and how they interact, the aim is to gain a comprehensive understanding of how relative humidity and temperature impact kitchen fronts. One potential outcome is that the testing period could be shortened by accelerating the test further, while still maintaining accurate results. This approach could allow for more tests to be carried out within the same timeframe, leading to the development of more efficient and reliable testing methods.

1.4 Delimitation

Medium-density fiberboards (MDF) are commonly used as carriers for IKEA's kitchen fronts. However, some product lines also use other materials like solid wood and particleboard. To protect kitchen fronts from humidity, they may be covered with foil, or coated with several layers of paint. Foil-wrapped fronts are entirely encased in plastic foil and edge banding, effectively blocking water vapor intrusion. Moisture can only infiltrate if there are gaps or damage to the foil. Painted fronts are not as resistant to humidity as the foil-wrapped fronts, but merely delay water vapor sorption to the carrier. Thus, painted kitchen fronts with MDF carriers were selected as the most suitable for this project.

To enable the fulfillment of this project, while still ensuring value for IKEA, a comprehensive analysis was conducted. This analysis compared sales data of different kitchen fronts against the proportion of total customer claims attributed to moisture defects. Due to the large volume of raw data, it was estimated that the majority of humidity-related claims could be categorized as surface issues. From this analysis, two different front families were selected, henceforth referred to as Front A and B, which differ in geometry but share similar carrier and coating materials. Figure 1.3 summarizes the sales data for the top four most sold painted kitchen fronts, denoted as A-D in Figure 1.3. It is evident from the figure that both Fronts A and B have significant sales volumes. Yet, they also exhibit a high proportion of customer claims related to humidity defects, thus it was concluded that the selection of these fronts was most suitable.

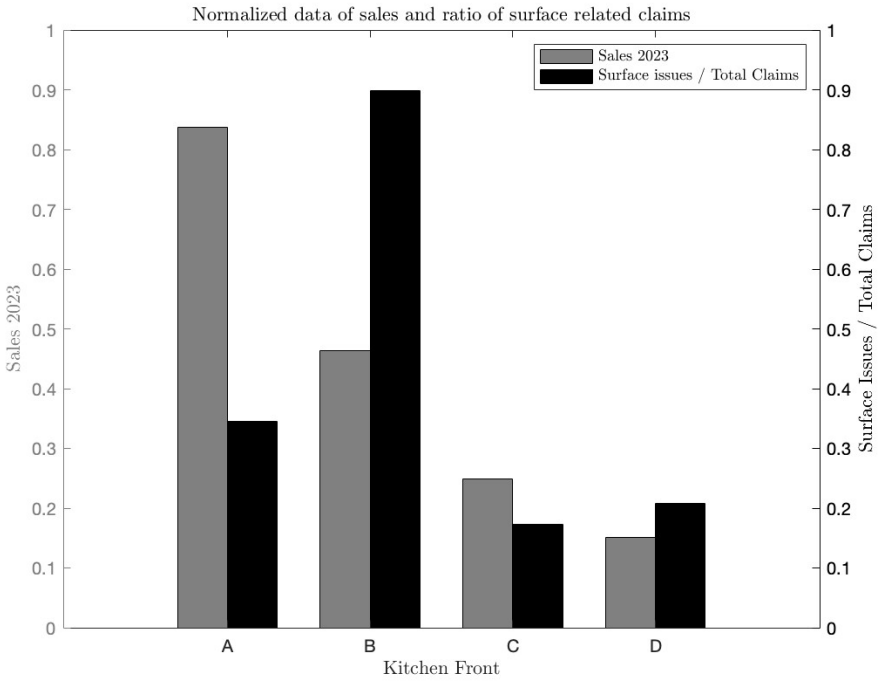

Figure 1.3: Normalized data of the four top-selling pigmented kitchen fronts where A and B represent the selected fronts. [1]

This thesis will only investigate changes in humidity caused by climate variations. Any humidity changes resulting from other sources, like steam from a dishwasher, will not be taken into account.

Chapter 2

Literature Review

This chapter will provide the theoretical foundation upon which later chapters of this thesis will be based.

2.1 Quality Management

Quality management is a fundamental concept in the industry that revolves around ensuring and continuously improving the product quality provided by a company. However, it might be difficult to define product quality. While some may argue that product improvement is connected to the fulfillment of certain pre-defined requirements, others emphasize a broader perspective, including improvements that optimize the overall experience and usability of the product. [15, 16]

A model that illustrates the relationship between customer satisfaction and the quality of a product is the Kano model, see Figure 2.1.

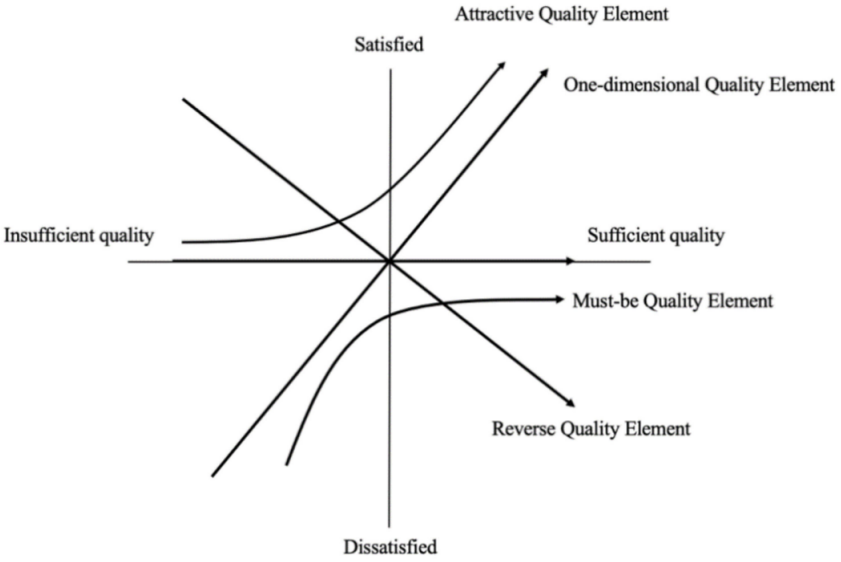

Figure 2.1: The Kano Model [2]

Figure 2.1 illustrates two key elements of product quality: Must-be quality elements and Attractive quality elements. Must-be quality refers to the minimum expected qualities or features of a product, while Attractive quality elements are those that customers may not initially anticipate or be aware of. It is crucial to meet the must-be quality requirements to ensure customer satisfaction. [15, pp. 28-29]

Implementing international standards like ISO 9001 for Quality Management Systems can help companies manage quality and customer satisfaction effectively and systematically. By integrating this standard into their organization and daily operations, companies ensure continuous improvements based on customer satisfaction and feedback. This approach assures customers that the company is committed to delivering high-quality products in a structured and proactive manner. [17]

2.2 Test Methods

Testing methods serve as foundational pillars in product development, ensuring the quality, durability, and safety of products. Doganaksoy

et al. [18] emphasize the critical role of product reliability in business success and the importance of testing methods in achieving this goal. These methods are crucial in evaluating product performance and verifying compliance with quality standards and regulatory requirements. Subjecting products to standardized tests can evaluate their performance under various conditions, such as mechanical stress, environmental exposure, and usage scenarios. Through systematic testing, potential weaknesses and flaws in product design or manufacturing processes can be identified early, enabling proactive measures to enhance product reliability and safety. Testing methods contribute to customer satisfaction by ensuring that products consistently meet or exceed expectations for quality, durability, and functionality.

2.2.1 Accelerated Testing

Accelerated testing is a process used to speed up the degradation rate of products and shorten their lifespan. This testing aims to obtain information quickly regarding the long-term performance of products with a long-predicted product life. There are different ways to achieve this objective, such as increasing the usage rate or overstressing the test sample. Increasing the usage rate can be done by running the product faster or reducing the off-time. Overstressing means that the product is subjected to higher loads than usual operating conditions. [19, pp. 3-4, 15-17]

It is also common to divide accelerated tests into two different categories with different purposes. They are sometimes called quantitative- and qualitative accelerated tests. The purpose of quantitative accelerated tests is to gather quantitative information about the life distribution or reliability of a product under accelerated conditions. By increasing factors such as temperature and pressure, the degradation or failure mechanism of the product being tested can be accelerated. Data is collected on the degradation under these accelerated conditions, and statistical models and analysis techniques are used to estimate the reliability under normal operating conditions. Understanding the relationship between the failure mechanism and the accelerated variables, based on chemical or physical theory, can help identify a model for extrapolation. On the

other hand, qualitative accelerated tests also involve increasing specific stress factors to accelerate product degradation, but the emphasis is on identifying failure modes, degradation mechanisms, and design weaknesses rather than obtaining quantitative reliability estimates. Data collected during these tests helps to identify and understand the underlying chemical or physical degradation process. It is important to investigate the root cause of failures in qualitative accelerated tests and assess whether the failure is reasonable and could occur in actual use. Setting stress factors too high during the tests may lead to unreasonable failure modes. [20, p. 2]

2.2.2 Product Failures

To improve the reliability of a product, it is essential to have a clear understanding of product failures and how they occur. According to Doganaksoy et al., [18, p. 53], product failures can be understood at three different levels, namely: "Failure mode", "Failure cause", and "Failure mechanism". The first level, "Failure mode", involves describing the observed indications of failure and how they affect the product. However, identifying failure modes is often not enough to resolve the underlying problems. The second level, "Failure cause", focuses on investigating the factors that led to a failure. Understanding the root cause of failure is crucial for implementing corrective measures and enhancing reliability. Finally, the third level, "Failure mechanism", aims to understand the fundamental physical or chemical process that led to a failure. This level is considered the ultimate goal in failure prevention.

Failure Mode and Effects Analysis (FMEA) is a helpful technique for identifying potential failures and reducing the risk of their occurrence. It is intended to provide critical information for making informed risk management decisions. According to Liu et al., [21, p. 829], it is crucial to accurately assess three key parameters — occurrence, severity, and detectability — to ensure effective risk prioritization. The occurrence is the probability that a failure will occur, severity is the impact that failure has if it occurs, and detectability is the likelihood of detecting the failure before it affects the customer or system. These risk factors are

then used to calculate the Risk Priority Number (RPN) of the failure modes to allocate the resources to address the most serious risk. RPN is calculated by multiplying the three risk factors:

$$RPN = O \times S \times D \tag{2.1}$$

The failure modes are then ranked based on their RPN score, and corrective actions are prioritized for the highest risk modes.

2.3 Design of Experiments

To study and understand a process and how the output depends on certain input factors, experiments are often used. Figure 2.2 represents a model of a general process. A process can be conceptualized as the degradation or ageing of a product, where factors such as temperature and humidity influence the measurable degradation of the product. An experiment, as defined by Montgomery [3, p. 1], is a series of tests that involve systematically varying input variables while observing output variables to determine their relationship. This structured approach enables the identification of which input variables are responsible for specific responses in the output variable. Additionally, experiments allow for the development of models that describe the relationship between input and output variables. This allows for the estimation of output variables under input conditions outside the tested range. [3, pp. 1-3]

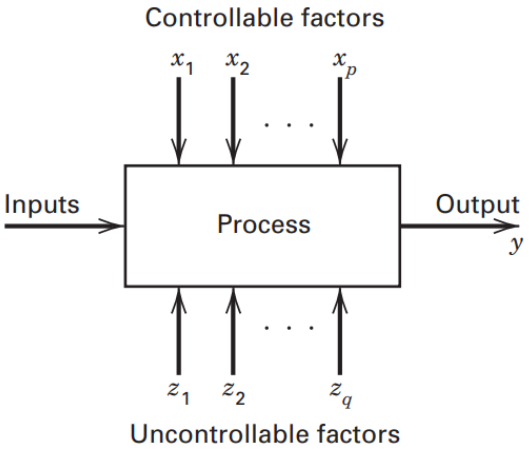

Figure 2.2: General model of a process [3, p. 3]

Design of experiments, as described by Montogomery, provides a structured methodology for conducting experiments. Montogomery recommends following the procedure presented in Table 2.1 below [3, pp. 14-21].

Table 2.1: Guidelines for designing and conducting an experiment [3]

1. Recognition and statement of the problem
2. Selection of the response variable
3. Choice of factors, levels, and ranges
4. Choice of experimental design
5. Performing the experiment
6. Statistical analysis of the data
7. Conclusions and recommendation

2.3.1 Factorial Design

Factorial design is an experimental design approach used to efficiently explore the effects of multiple factors on a response variable. It allows for the study of the main effects and their interactions. According to Montgomery, factorial designs are generally the most efficient for experiments involving two or more factors [3, p. 183]. In factorial designs, the levels of the different factors are systematically varied to observe the

impact on the response variable. When designing an experiment, the number of levels for each factor must be carefully considered. Increasing the number of levels provides higher resolution, allowing for a more precise estimation of main effects and interactions. However, a higher number of levels will drastically increase the number of tests required within the experiment.

Factorial design uses the notation 2^k to represent a two-level design with k number of factors. These factors may be continuous, such as temperature, or discrete, such as the number of operators involved in a process. Generally, the high and low levels of each factor are denoted as 1 and 0, respectively. The simplest factorial design analyzes two factors, A and B, denoted by $k = 2$. Thus, such a design measures how the response variable varies across four different combinations of A and B. The principal look of such a design, along with the different combinations of A and B, is shown in Figure 2.3. [3, pp. 233-234]

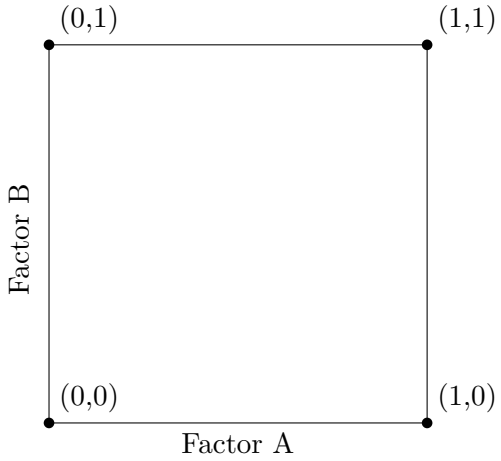

Figure 2.3: 2^2 factorial design

If three levels of each factor are of interest, the notation will be 3^2. The different levels of such a design are referred to as low, intermediate, and high. Similarly to the 2^2 example above, these levels are denoted by -1, 0, and 1, respectively. A three-level factorial design allows for the exploration of a potential non-linear relationship between the controlled

and measured variables. An example of such a factorial design is shown in Figure 2.4. [3, pp. 395-396]

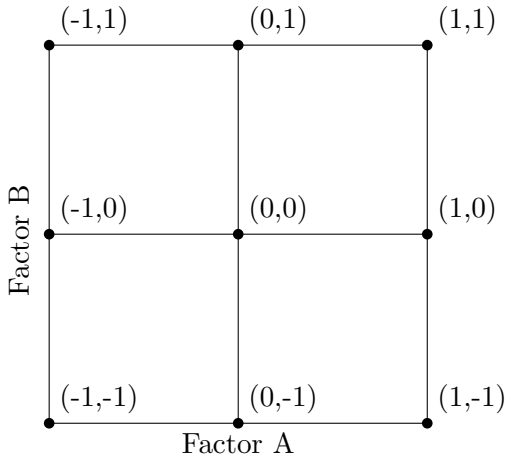

Figure 2.4: 3^2 factorial design

These types of factorial designs, i.e. 2^2 and 3^2, not only allow for the analysis of how the two factors impact the dependent variable but also how they interact with each other and how this interaction affects the dependent, i.e. measured, variable.

2.4 Measurement

Measurement refers to the act of quantifying physical phenomena through the utilization of measuring instruments [22, p. 1]. It is an essential and fundamental aspect of scientific inquiry, as it provides the means of quantifying and validating observations systematically and accurately. However, it is important to keep in mind that all measurements are prone to errors and uncertainties, which can impact the accuracy and reliability of experimental results. The precision of the measuring instrument, the methodology used, and the expertise of the experimenter influence the accuracy of a measurement [22, p. 18]. Therefore, it is crucial to consider these factors when conducting research to ensure the accuracy of scientific findings.

2.4.1 Sources of Errors and Uncertanties

The true value of a measurable quantity is always unknown, and the measurement is just an estimation of the true value [22, pp. 20]. Therefore, the estimation of measurement errors is necessary. Measurement errors are often distinguished between random and systematic errors, where random errors are unpredictable fluctuations in measurement readings that occur randomly, and systematic errors result from consistent inaccuracies or biases in measurement readings. Measurement errors and uncertainties can arise from various sources, including methodological, instrumental, and personal errors. The total measurement error, denoted as ζ, can be expressed as the sum of individual errors associated with each component and its imperfections

$$\zeta = \zeta_m + \zeta_i + \zeta_p \tag{2.2}$$

where ζ_m, ζ_i, and ζ_p represent the methodological, instrumental, and personal errors, respectively [22, p. 20].

2.5 Medium-Density fiberboard

Fiberboard is a material that originated from the paper industry and was first produced on a large scale in the late 1800s. Medium-density fiberboard, also known as MDF, is a type of fiberboard, see Figure 2.6a. It is made by mixing wood fibers (see Figure 2.5 for reference) and adhesives, which are then compressed by plates, with the application of heat. The small wood fibers present in MDF make the material homogeneous and thus suitable for machining processes, such as milling. Due to these material properties, MDF is commonly found within the furniture industry, such as in the manufacturing of kitchen fronts. [23, 24]

Figure 2.5: Wood fibers used for MDF [4]

(a) MDF **(b)** Particle Board

Figure 2.6: Medium Density fiberboard (MDF) and Particle Board [5, 6]

Due to the membrane pressing the wood fibers and adhesive together, the fibers are mainly oriented in the direction of the board. This orientation is illustrated in Figure 2.7 below, which clearly depicts how dense and homogenous the material is and thus makes it suitable for machining. [23]

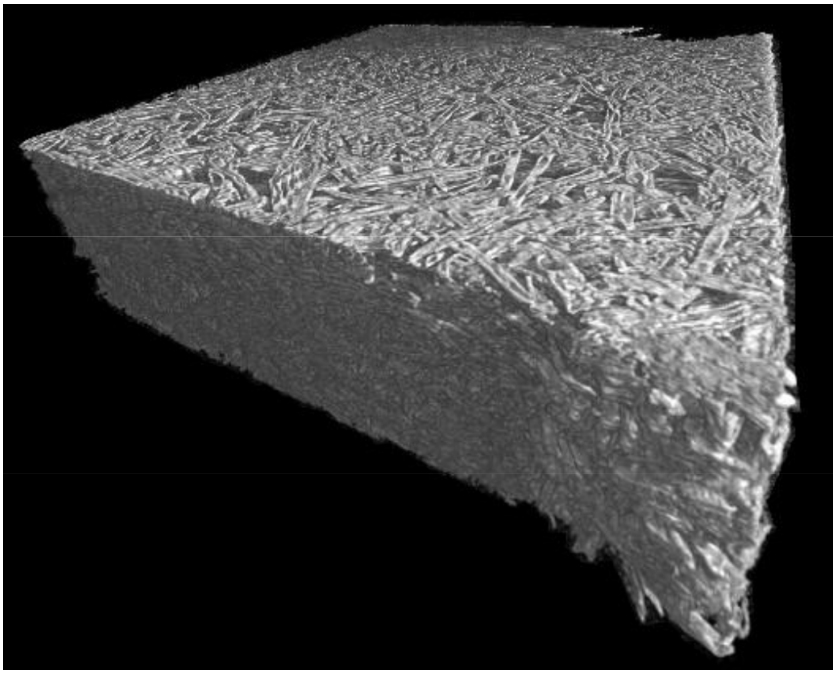

Figure 2.7: MDF-board [7]

However, a significant drawback of MDF is its sensitivity to moist and humid climates, which causes swelling, predominantly in the thickness direction of the board. This swelling occurs primarily in the thickness direction because the wood fibers expand perpendicular to their orientation when exposed to moisture. [7, 23, 25]

2.6 Humidity

2.6.1 Relative Humidity and Humidity Ratio

Relative humidity (φ) is a widely used measurement in various fields, such as meteorology, construction, and material science. It provides a quantitative measurement, between 0 and 1, of how close the surrounding air is to being saturated. Since hot air can hold larger amounts of water vapor, the measurement is thus temperature-dependent, demonstrating an inverse relationship between temperature and φ. This relationship can be defined as

$$\varphi = \frac{v}{v_s(T)} \tag{2.3}$$

Or

$$\varphi = \frac{P_w}{P_{sat}(T)} \tag{2.4}$$

where P_w and P_{sat} are the partial water vapor pressure and saturated vapor pressure, respectively. v is the actual vapor content and $v_s(T)$ is the saturation vapor content, i.e. the maximum amount of vapor content that the air can hold until it is fully saturated, causing excess water vapor to condense. [23, 26, pp. 328-329, p. 78]

It should be stressed that φ is not a measurement of the total water vapor mass in the air, instead, it quantifies how close the current water vapor mass is to its maximum, i.e., saturation [27, p. 376]. However, there is a measurement that specifically quantifies the ratio of water vapor mass to dry air mass. This measurement is known as the humidity ratio (ω) and can be defined as [27, pp. 376-377]

$$\omega = \frac{m_w}{m_a} \tag{2.5}$$

where m_w is the water vapor mass and m_a is the mass of the dry air.

However, a distinct relationship exists between φ, ω, and the temperature of the air, commonly referred to as the dry bulb temperature. This relationship can be illustrated by a psychrometric chart as shown below in Figure 2.8.

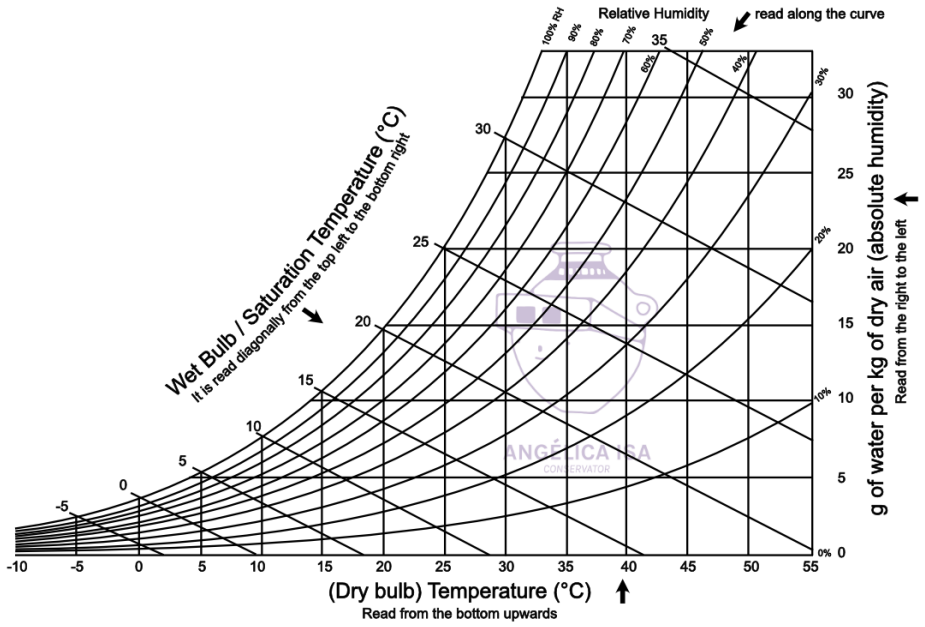

Figure 2.8: Psychrometric chart, φ is shown in % [8]

The chart demonstrates that air with higher temperatures can hold a larger amount of water vapor. The chart also indicates that significant changes in the air temperature can cause the excess water vapor to condense. If two variables are known, the chart can be used to determine any other variable on the chart.

From the preceding discussion, as well as the psychrometric chart shown in Figure 2.8, it is reasonable to assume that the ω can be expressed as a function of φ and, consequently, the surrounding air temperature. This expression can be derived from Equation 2.5, which states that

$$\omega = \frac{m_w}{m_a}$$

m_w and m_a can also be expressed as the number of moles (N) and the molar mass (M), respectively. Equation 2.5 can then be rewritten as [27, p. 376]

$$\omega = \frac{N_w M_w}{N_a M_a} \tag{2.6}$$

The ideal gas law states that the ratio of the number of moles of two gases in an ideal gas mixture can be expressed as [27, p. 374]

$$\frac{N_w}{N_a} = \frac{P_w}{P_a} \tag{2.7}$$

where P_w and P_a are the partial pressure of water vapor and air. By looking up P_w and P_a and inserting equation 2.7 into 2.6, one gets [27, 28, p. 1381, p. 377]

$$\omega = 0.622 \, \frac{P_w}{P_a} \tag{2.8}$$

Dalton's law can be used to find the total partial pressure, which in this case is [27, p. 373,377]

$$P = \sum_{i=1}^{n} P_i = P_w + P_a \tag{2.9}$$

By using Dalton's law, along with equation 2.8, one gets

$$\omega = 0.622 \, \frac{P_w}{P - P_w} \tag{2.10}$$

Equation 2.4 can be rewritten as $P_w = \varphi P_{sat}(T)$. By using this relationship, along with 3.1.6, we get an expression for ω and how it relates to temperature and φ [27, p. 377]

$$\omega = 0.622 \, \frac{\varphi P_{sat}(T)}{P - \varphi P_{sat}(T)} \tag{2.11}$$

This relationship allows a clear comparison of water vapor in dry air between different settings of φ and temperature.

2.7 Humidity Impact on Wood

Wood materials feature small openings known as pores, which allow for the movement of moisture within the material. This transport of moisture into, and within the material, can be driven in two ways; capillary forces or sorption (adsorption and desorption). [29]

When capillary forces are present, water transport occurs when wood directly encounters water, drawing it into the material through these narrow openings. This fluid motion can result in material expansion, potentially leading to the development of cracks in applied coatings, such as painted or foiled coatings. [10, 23]

Furthermore, the moisture transport can also be caused by sorption, i.e. humidity gradient between the wood and the surrounding air. The material consistently seeks to align its humidity content with that of the surrounding air; this is known as the equilibrium moisture content (EMC) and can be expressed as

$$w_e = \frac{m_w - m_{dry}}{m_{dry}} \tag{2.12}$$

where m_w and m_{dry} are wet and dry mass of the specimen, respectively. [24, p. 359]

Similar to the principles of heat transfer, this implies that the material has the ability to both desorb and absorb water vapor, depending on the relative humidity of the surrounding air. Thus, w_e of a material is dependent on the relative humidity of the surrounding air. [23, 24]

When measuring and graphing the w_e at various levels of relative humidity, a curve known as the sorption isotherm is obtained. This curve illustrates both the desorption and adsorption of a wooden material at different levels of relative humidity [24]. An illustrative example of such a sorption isotherm is presented below, see Figure 2.9. Please note that the specific characteristics of the sorption isotherm curve will be dependent on the particular material. Nevertheless, Figure 2.9 provides a representation of the typical appearance of the curve, showing w_e as a function of φ. The curve in Figure 2.9 is for aspen material [9]. Hence, the magnitude of the y-axis (w_e) should not be considered.

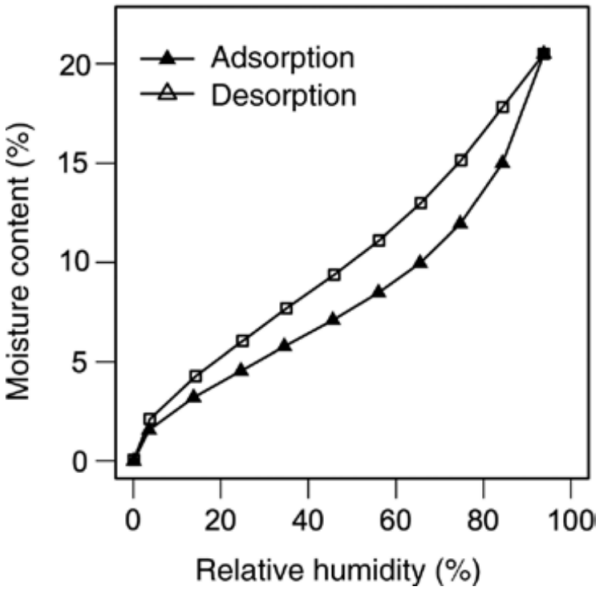

Figure 2.9: Sorption isotherm [9]

In this graph, the measurements taken during both absorption and desorption are illustrated. The graph shows that moisture adsorption and desorption follow different paths. It should also be stressed that these curves are measured during constant temperature, hence the name sorption isotherm [23, p. 86]. The slope of the curve, at any point, is referred to as the moisture capacity (ξ) and can be expressed as [26, p. 251]

$$\xi = \frac{dw_e}{d\varphi} \tag{2.13}$$

ξ is thus a measurement of how much w_e changes with φ. From Figure 2.9, it can be concluded that ξ is largest at low- and high values of φ.

Figure 2.9 shows a non-linear curve derived from experimental data. However, some studies have applied Nelson's sorption isotherm as a theoretical model and compared it with experimental data to evaluate its accuracy. According to [30], the sorption isotherm is temperature-dependent, where a higher temperature will result in a lower w_e. However, if different sorption isotherm curves are plotted in the same figure

with various temperatures, using the equation presented by [30], it can be concluded that the temperature's effect on the equilibrium moisture content will be negligible within certain intervals of φ, as shown in Figure 2.10.

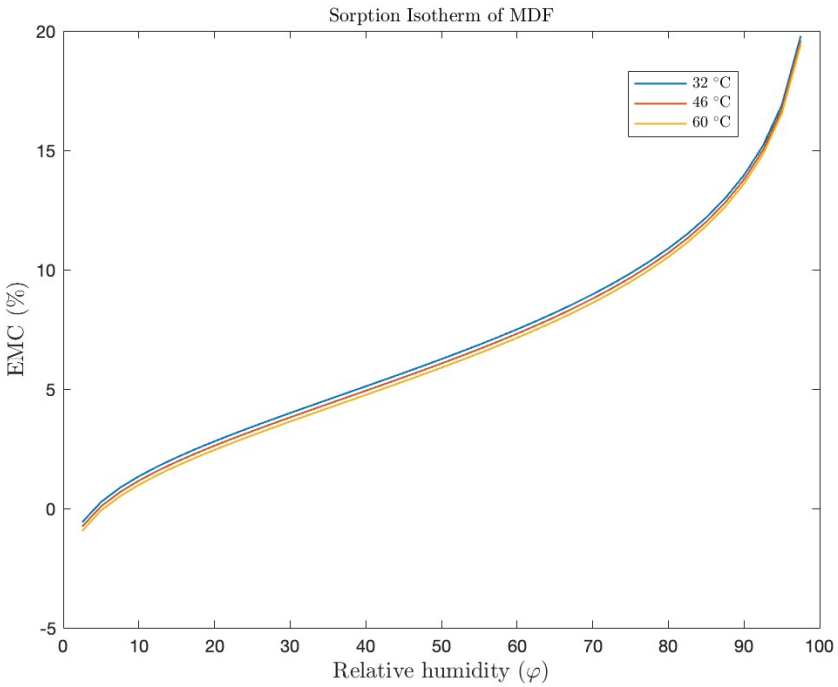

Figure 2.10: Sorption isotherm for MDF at various temperatures

Figures 2.9 and 2.10 show the sorption curve for wood, with the second figure depicting the sorption curve for an MDF board. In these plots, the equilibrium moisture content (w_e) is plotted against various levels of relative humidity, φ. However, as shown in Figure 2.9, the material will release moisture if it has a higher moisture content than the surrounding air. When the desorption curve deviates from the adsorption curve, it is referred to as hysteresis. [26]

2.7.1 Moisture Diffusion in Wood

To enable moisture diffusion within a material, a gradient must be present. Considering that this report will focus on humidity and its

impact on kitchen fronts, the gradient, in this case, will be in the form of a difference in vapor content, i.e., Δv. For the case of stationary moisture diffusion (g) through a material, the following expression can be applied [10]

$$g = -\delta_v \frac{dv}{dx} \tag{2.14}$$

where δ_v is the water vapor permeability coefficient.

The coefficient δ_v is dependent on the value of φ and the temperature of the surrounding air. An increase in both φ and temperature will lead to a larger value of δ_v [31]. Consequently, in accordance with Equation 2.14, this will result in faster moisture diffusion throughout the wood [10, pp. 331-333].

The negative sign preceding the expression accounts for the fact that moisture diffusion always moves from areas of high concentration to areas of low concentration, thus making Δv negative. This stationary diffusion through a single layer material is shown in Figure 2.11 below.

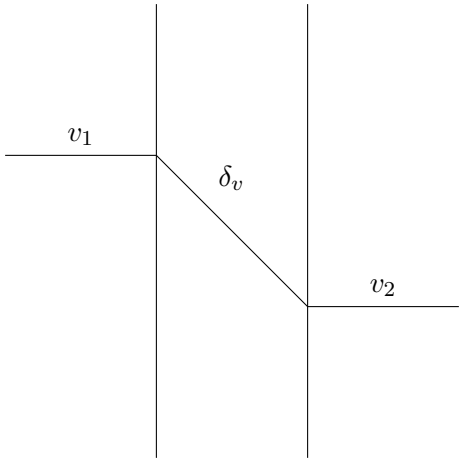

Figure 2.11: Stationary moisture diffusion through one layer [**?**]

However, there may be multiple layers within the material of interest, such as coated wood. When the thickness of these layers is known, the vapor transmission resistance, denoted as Z, is applied. In cases

where the layers are thin, this resistance is commonly utilized. The transmission resistance can be expressed as [10]

$$Z = \frac{d}{\delta_v} \tag{2.15}$$

where d is the thickness of the layer.

Similar to Figure 2.11 the moisture diffusion can be illustrated through several layers. Just as with Figure 2.11, the flow will be from areas of high concentration to low concentration, indicated by a negative slope in Figure 2.12.

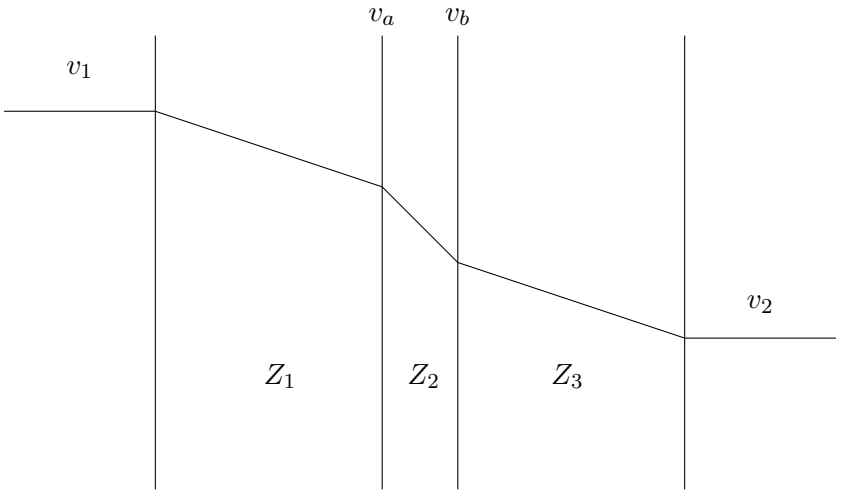

Figure 2.12: Moisture diffusion through several layers [10]

If several layers are present and Z_n are known, the vapor content at the different layers, e.g. v_a and v_b in Figure 2.12, can be calculated.

Figures 2.11 and 2.12 assume a difference between v_1 and v_2 as the driving force behind moisture flow. However, if no gradient is present, i.e., $v_1 = v_2$, moisture movement will still occur, provided that the moisture content in the middle of the specimen is not in equilibrium with the surrounding air. In such a scenario, the moisture flow will be symmetrical, as indicated by Figure 2.13.

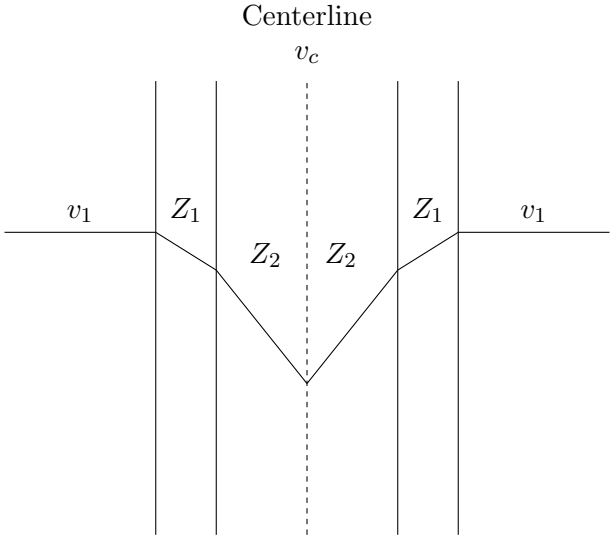

Figure 2.13: Stationary moisture diffusion through several layers

2.8 Temperature Impact on Coating

It has been demonstrated that several chemical reactions display an exponential correlation with temperature, where higher temperatures result in an accelerated reaction rate. A widely used model to describe the influence of temperature on a reaction is the Arrhenius model, typically expressed as follows:

$$R(\text{temp}) = \gamma_0 \exp\left(\frac{-E_a}{k \cdot T(K)}\right) \tag{2.16}$$

where R is the reaction rate, γ_0 is the pre-exponential factor, E_a is the activation energy, k is the Boltzmann's constant, and $T(K)$ is the temperature in kelvin. [20, p. 10]

2.16 clearly illustrates how the rate of reaction is significantly influenced by temperature, as it enhances the kinetic energy of molecules, thereby accelerating the reaction rate. Consequently, fluctuations in ambient temperature will greatly affect the speed at which water molecules are transported through protective coatings. Therefore, establishing a fundamental understanding of the environmental temperature in which the product will operate is crucial. [32]

Chapter 3

Methodology

The methodology chapter acts as a roadmap for achieving the thesis objectives by outlining the approach, steps, and motivation behind the main decisions during the project.

3.1 Method Overview

In this section, the main steps for achieving the aim and purpose of this thesis will be presented in chronological order. Initially, the steps will be presented in the form of a flowchart, see Figure 3.1, to get an easy overview of the steps which will be presented in further detail in Subsection 3.1.1 - 3.1.6 below.

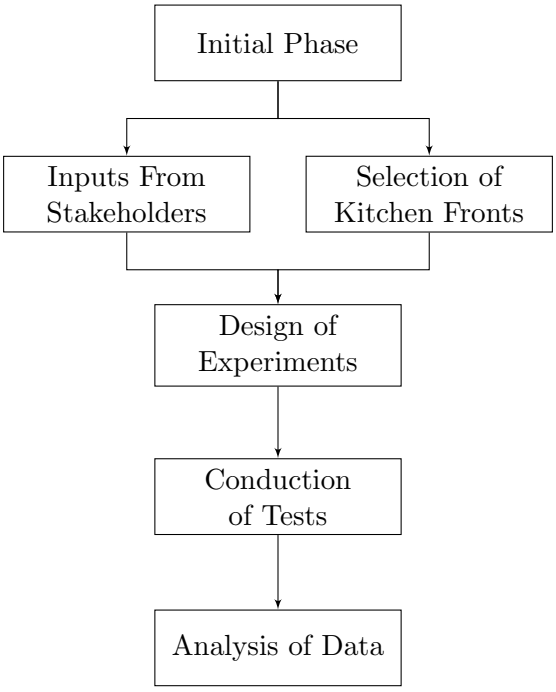

Figure 3.1: Flowchart of the methology

3.1.1 Initial Phase

During the initial phase of the project, the main objective was to gain an overview of the project, as it was initially extensive and quite diffuse. Thus, the primary task during the initial phase was to narrow down the project and adapt it to the scope of this thesis. Information regarding the production process of kitchen fronts in Älmhult was also compiled and a tour of the production site was given.

3.1.2 Inputs From Stakeholders

To gain a broader understanding of the different types of kitchen fronts available and the methods currently used to test them, several stakeholders at IKEA were contacted. These stakeholders were experts in various relevant areas such as MDF carriers, surfaces and coatings, and humidity problems in wooden furniture, among others.

Unstructured interviews were chosen as the primary method for gath-

ering information, as this approach allowed for a more natural type of conversation and encouraged participants to share their insights freely and spontaneously. Initial contacts were provided by the supervisor at IKEA, but during the interviews, participants often referred to other relevant experts, expanding the number of interviewees.

The selection of participants was based on their expertise and relevance to the project. Interviews were conducted in informal settings, such as their offices or meeting rooms at IKEA, to encourage open and free discussions. Each conversation lasted approximately 30 to 60 minutes, depending on the availability and engagement of the participant.

During the interviews, the project and its aims were initially presented to collect valuable input based on the previous knowledge and experience of the stakeholders. Minor notes were taken continuously to capture essential information and insights.

Given that conducting tests in a climate chamber is time-consuming, it was crucial to choose kitchen fronts that would allow us to complete all tests within the required timeframe. The fronts wrapped in foil are more resistant to moisture transport, which means it would take longer to see results from the tests. As a result, after discussions with relevant stakeholders, it was decided that the selected fronts for the project should have a painted coating.

3.1.3 Selection of Kitchen Fronts

Concurrently with gathering information from stakeholders, an analysis of sales volume and customer claims for kitchen fronts was conducted. The selection of fronts was briefly introduced in Section 1.4 and illustrated in Figure 1.3, aiming to provide an overview of the ratio between humidity-related claims and the total number of claims. This analysis assumed that a significant portion of surface-related issues derived from humidity. Since this project aimed to generate valuable insights for IKEA, the selected kitchen fronts needed to be popular items with substantial sales volumes. Therefore, normalization of the collected data

was conducted to enable a meaningful comparison of factors with differing scales, i.e. the ratio of claims and sales volumes. The conclusions drawn from this analysis, combined with stakeholder inputs, see subsection 3.1.2 above, formed the basis for the selection phase.

Additionally, given IKEA's presence in diverse global markets with varying climates, comparing any variations and differences in quality between suppliers was of interest. To facilitate reliable comparisons between production sites, the same fronts were chosen from both suppliers.

3.1.3.1 Front A and B

As mentioned briefly in Section 1.4, fronts A and B differ in geometry and colour. Front A has a simple geometry with a flat surface, while front B has a more complex geometry with a milled surface. These differences in geometry lead to variations in the density profiles of the MDF board, where front B requires a higher density closer to the surface to allow for milling. Additionally, the two fronts differ in thickness, with front A having a thickness of approximately 16 mm, while front B has a thickness of approximately 19 mm. Both surfaces are coated with layers of polyurethane and acrylic paint. The lacquer system for the fronts manufactured in Asia is different from those manufactured in Europe.

3.1.4 Design of Experiment

The steps in Table 2.1 served as a foundation when designing the experiment. The recognition and statement of the problem were initially identified; i.e. how different parameters of humidity and temperature impact the quality of the kitchen fronts. Since the humidity-related issues could be derived from the sorption of water vapor into the carrier of the kitchen fronts, the percental weight increase was selected as the response variable because it is easily quantified and measurable. The scale used to weigh the kitchen fronts had a $\pm$ 2 g tolerance and was regularly controlled and calibrated with calibration weights. Even though 2 g is approximately 0,07 % of the total weight of the fronts, it could affect the accuracy of the weight increase for the fronts that did not gain

that much weight. Initially, the thickness of the carriers was measured with a micrometer. However, as a result of the absorbed water vapor, the carriers became spongy and consequently the measurements became unreliable. A conclusion was reached that the error associated with the thickness measurement was too large. Therefore, these measurements were not used in the analysis.

In Subsection 2.3.1, the theory behind factorial design was presented. For this project, the two factors to be considered are temperature and relative humidity. The selected parameters for these factors were based on the currently used parameters at IKEA (32/90), as well as the highest temperature and humidity levels observed at the end customer's homes. As outlined in the background, see Section 1.1, the most challenging environment occurs during transport and storage, where temperature levels of 60°C and relative humidity levels of 70-95 % could be seen. These levels were used as a worst-case scenario when selecting the design points. Although it is unrealistic to attain a temperature of 60°C and relative humidity of 95 % simultaneously in practice, this extreme scenario was used to potentially accelerate the weight increase even further, as it also was of interest to decrease the required testing period. Relative humidity higher than 95 % could not be used because it is close to the saturation point of the air, which may lead to condensation in the climate chamber. However, increasing the relative humidity level from the current testing parameter of 90 % to 95 % leads to an exponential increase in the saturation point of the MDF board as presented in Section 2.7.

The selected levels of temperature and relative humidity for the fronts from the European supplier are shown in Figure 3.2. Figure 3.3 presents the selected design points for the fronts from the Asian supplier.

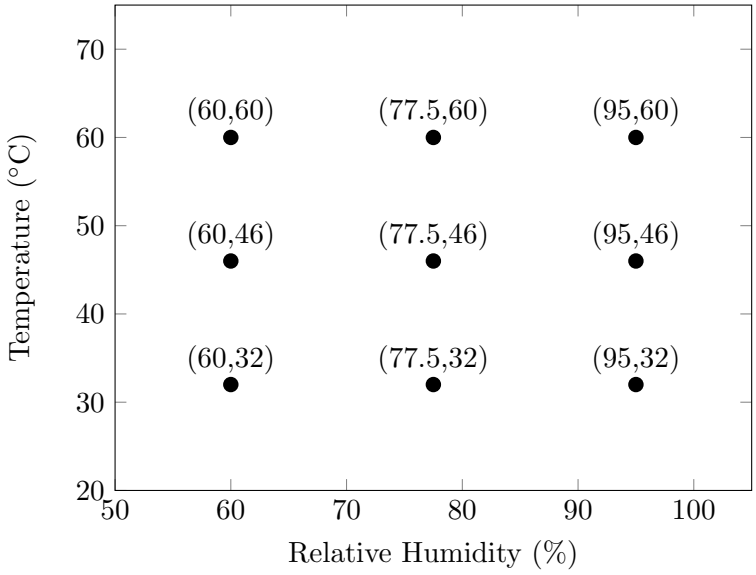

Figure 3.2: Selected design points

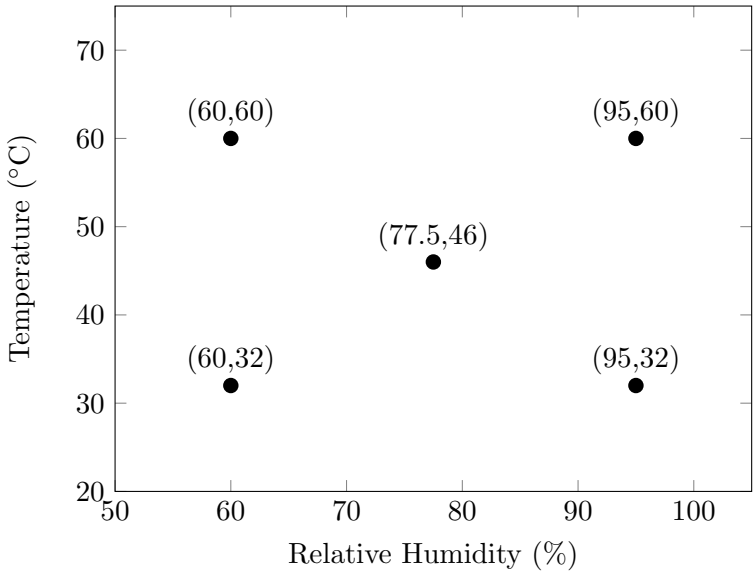

Figure 3.3: Design points for the fronts from the Asian supplier

As shown in Figure 3.2, three levels of each factor were selected, and thus a 3^2 factorial design was conducted. Due to delays in the supply chain from the Asian supplier, these fronts could not be included in

all of the conducted tests, as depicted in Figure 3.3. Consequently, the tests corresponding to intermediate levels of relative humidity and temperature were not carried out with fronts from both suppliers. The tests corresponding to the corners in Figure 3.3, were saved to facilitate the inclusion of fronts from both suppliers, aiming to explore as wide of a design window as possible. Thus, forming a 2^2 factorial design with a centerpoint. When gathering inputs from the stakeholders within IKEA, it was concluded that the relationship between the dependent and non-dependent variables was likely non-linear. Following the theory presented in Subsection 2.3.1, a 3^k was thus most suitable, as it allows for the identification of a non-linear relationship between the dependent and independent variables, which would not be possible with a 2^k factorial design.

3.1.5 Conduction of Tests

As previously mentioned, the experiments were conducted in climate chambers (see Figure 3.4 for reference), which provided precise control over temperature and humidity. Each chamber could accommodate up to 15 kitchen fronts, with three fronts of each type being tested simultaneously to minimize the impact of random variations. To clarify, each test contained three fronts of front A from both the European and Asian supplier, three fronts of front B from both suppliers and three uncoated MDF boards (carriers) from the European supplier. Before the placement in the climate chamber, the kitchen fronts were housed in a room with constant temperature and humidity conditions, to ensure that all fronts reached equilibrium before testing. Once equilibrium was attained, the kitchen fronts were transferred to the climate chamber, where they were placed vertically ($90° \pm 5°$) in a rack. The duration of the tests was approximately 330 hours, allowing for the completion of all required tests within the time frame. Throughout each testing period, the weight of every kitchen front was measured at regular intervals.

Figure 3.4: Climate chamber

Data on temperature and relative humidity are collected at regular intervals, typically several times per minute, from climate chambers similar to the one depicted above. This data is then plotted throughout the test period to provide an overview of any potential deviations, as illustrated in Figure 3.5. By referencing Figure 3.5, one can determine instances when the climate chamber was opened, indicated by drops and overshoots in relative humidity (φ).

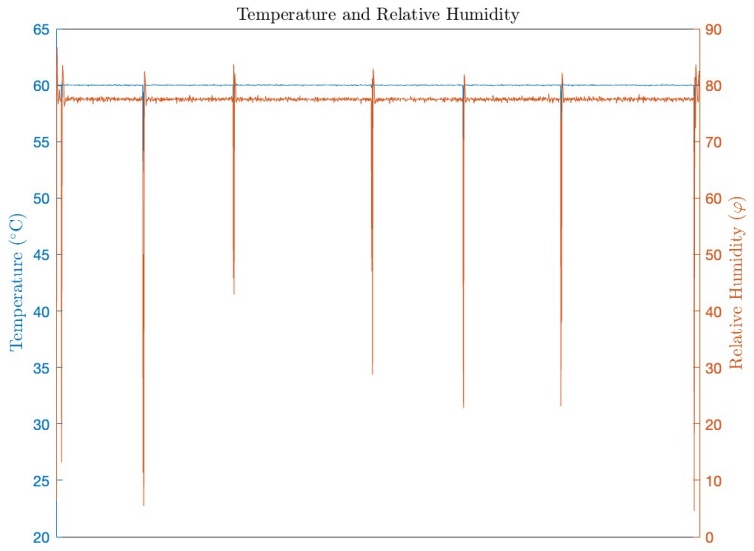

Figure 3.5: Temperature log from the climate chamber at 60°C and 77.5 φ

Plots similar to the one above can be found in Appendix A for all of the tests, see Figure A.1 - A.10.

3.1.6 Analysis of Data

Finally, when all tests were conducted, the collected data could be analyzed and conclusions could be drawn. To verify that the relationships were statistically significant, an ANOVA analysis was carried out using the R-language in RStudio. For all plots in this thesis, MATLAB was used while Excel served as a database of the measurements upon which the plots are based.

Chapter 4

Results and Discussion

In this chapter, the study's findings will be presented to provide an overview of the empirical data collected and analyzed. The experiment involved subjecting an uncoated MDF board - carrier, and two different kitchen fronts - A and B, to varying temperatures and relative humidity in a climate chamber.

The chapter will begin with a summary of the study's results and descriptive statistics, followed by a detailed presentation of the findings for the carrier and each of the fronts.

4.1 Overview of Results

The primary focus of the investigation was to analyze the weight gain of kitchen fronts in response to changes in relative humidity and temperature. The results revealed a consistent trend across all tested samples, where an increase in relative humidity corresponded to a significant increase in weight gain for all kitchen fronts. This finding aligns with previous research indicating that higher relative humidity levels promote moisture absorption in porous materials such as MDF.

The results also revealed a positive correlation between weight increase and temperature for front A and B, while the carrier showed different behavior. This discrepancy can be attributed to the influence of the

temperature on the coating as described in the Theory section. Based on previous studies, the temperature has a negative impact on the EMC, which explains the result for the carrier. However, the temperature increased the rate of weight gain for both the uncoated and coated carriers.

Another noteworthy observation from the study was the saturation behavior of the kitchen fronts under investigation. The carrier consistently approached saturation across almost all tests, indicating rapid moisture absorption and reaching its saturation point within the experimental timeframe. In contrast, front A and B did not reach a stationary weight value during the duration of the experiments in all of the conducted tests. This phenomenon can be attributed to the presence of a protective coating on the surface of the coated MDF boards, which acts as a barrier to moisture absorption and slows down the rate of weight gain. Consequently, the weight increment for coated MDF boards takes longer to stabilize compared to uncoated counterparts.

4.2 Descriptive Statistics

Initially, the fronts from both European and Asian suppliers were weighed, and the data were compiled. This step aimed to facilitate the identification of potential deviations in the tests, particularly in the inputs, i.e. the mass of the carrier and the fronts. Additionally, it allows for tracing how weight may correlate with thicker coating, and thus greater resistance to moisture and its ability to penetrate through the coating by diffusion. The data is compiled below, see Table 4.1 and 4.2 with corresponding boxplots in Figure 4.1 and 4.2

Table 4.1: Descriptive Statistics From European Supplier

	Kitchen front		
	A	B	Carrier
$\bar{x}$ (g)	2870.9	3410.9	2771.7
Q_1 (g)	2826	3400	2760
Q_2 (g)	2886	3415	2770
Q_3 (g)	2898	3418	2786
σ (g)	42.0205	17.5753	16.7639
n	30	30	30

Table 4.2: Descriptive Statistics From Asia Supplier

	Kitchen front	
	A	B
$\bar{x}$ (g)	2992	3447.3333
Q_1 (g)	2988	3444
Q_2 (g)	2992	3447
Q_3 (g)	2996	3452
σ (g)	6.2497	5.573
n	18	18

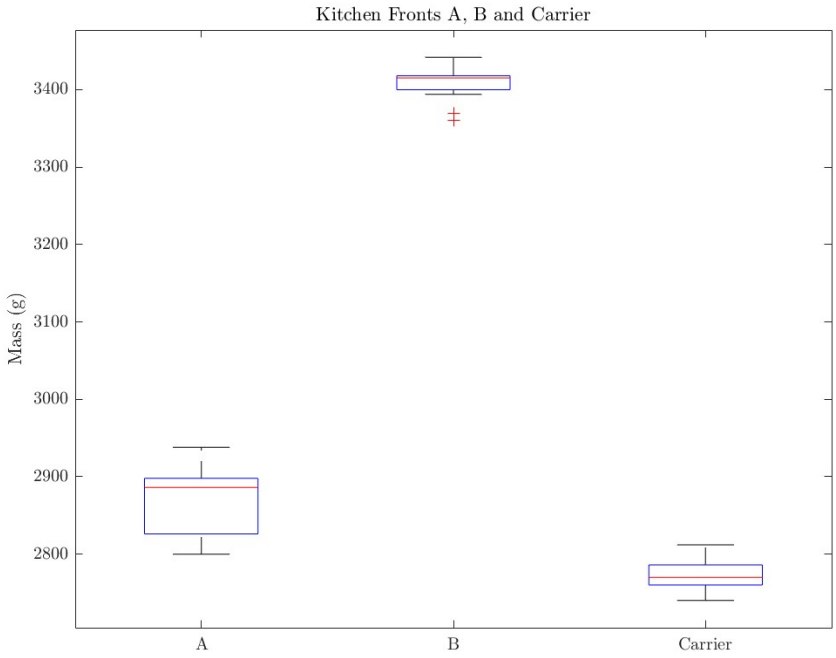

Figure 4.1: Boxplot of kitchen front A, B and Carrier from European Supplier

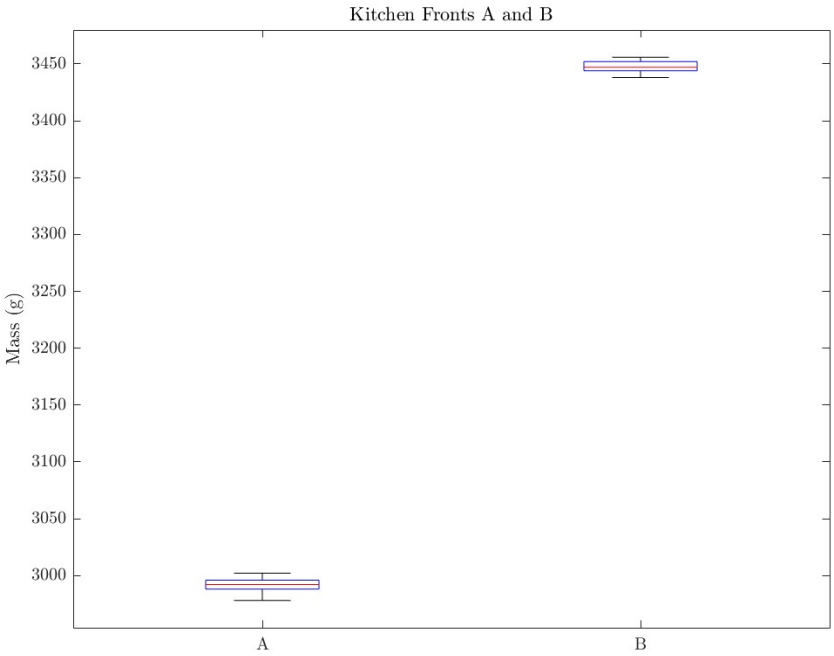

Figure 4.2: Boxplot of kitchen front A and B from Asia Supplier

4.3 Carrier

As stated in the Methodology chapter, the fronts and carrier were placed in the climate chamber for approximately 330 hours, which allowed for the completion of all test series. Figure 4.3 presents the total weight increase observed over the test period, with the temperature and relative humidity levels currently implemented at IKEA highlighted by the red bar. The levels of temperature and relative humidity will henceforth be written as 'temperature/relative humidity', e.g. '32/95'.

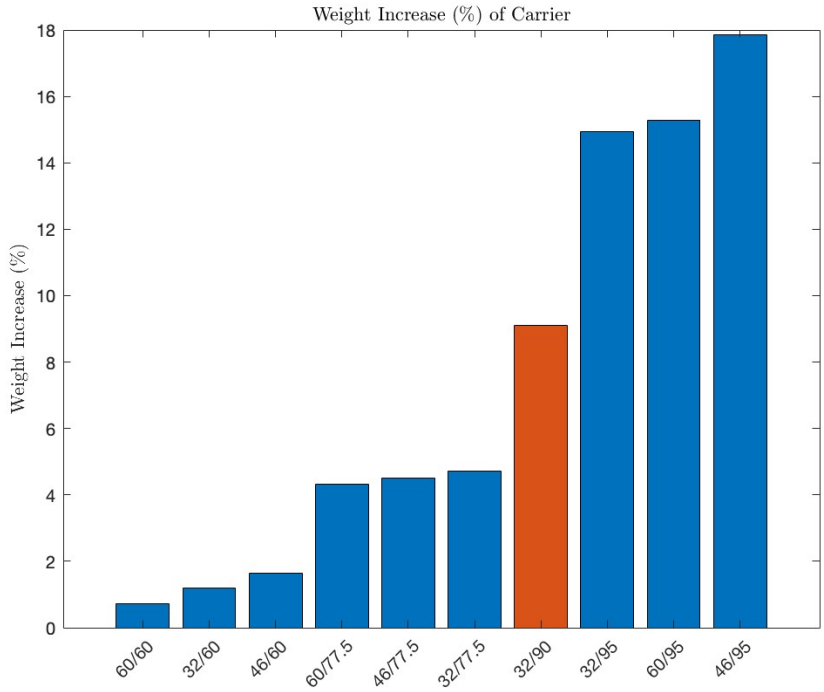

Figure 4.3: Total weight increase of carrier (%) after ∼330 h

The order of the bars in Figure 4.3 corresponds to the theory discussed in Section 2.7. According to this theory, a higher relative humidity of the surrounding air will result in higher water vapor absorption into the wood. This is also supported by the sorption isotherm shown in Figure 2.10, which depicts an exponential increase in EMC when entering regions with high relative humidity values. Specifically, there is a large increase of Δm when entering higher regions of relative humidity ($>$ 90%), resulting in a high value of the moisture capacity (ξ), see Equation 2.13.

It should be noted that the sorption isotherm curve displays an inverse relationship between the EMC and the temperature of the surrounding air. This means that as long as the relative humidity remains constant, the EMC decreases as the temperature increases. However, this contradicts the order of the bars in Figure 4.3, which should be arranged in the order of 60, 46, and 32 °C for each level of relative humidity, according

to Figure 2.10. This inconsistency can be explained by the water vapor permeability (δ_v) being temperature-dependent, resulting in faster diffusion throughout the material at higher temperatures. Therefore, tests conducted at higher temperatures will reach saturation, i.e. converge toward a stationary value and stabilize faster. To demonstrate the impact of temperature on the weight increase, or the rate of diffusion, the parameters corresponding to the three bars with 95 % relative humidity in Figure 4.3 can be plotted over time, see Figure 4.4.

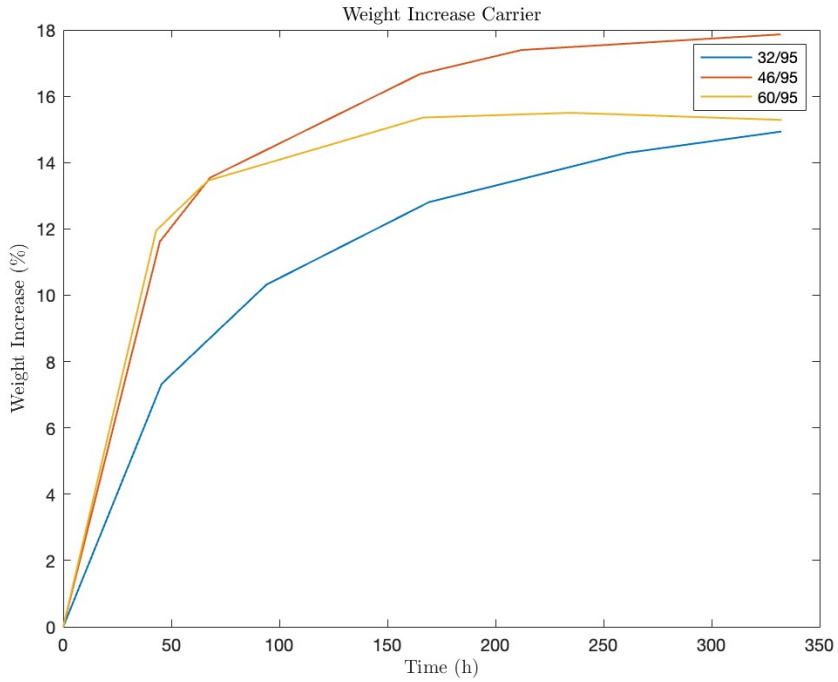

Figure 4.4: Weight increase of carrier at constant relative humidity and varying temperature

The graph depicts the weight increase of three different lines in varying temperatures and a constant level of relative humidity. The yellow line, representing 60/95, shows a clear convergence in weight increase after approximately 160-170 hours. On the other hand, the blue and red lines continue to gain weight without converging towards a stationary value even after approximately 330 hours.

However, it is desired to include plots illustrating the weight increase over time for all nine different combinations outlined in the Methodology chapter (see Subsection 3.1.4 and Figure 3.2 - 3.3). In contrast to Figure 4.4, where the relative humidity remains constant, the following figures depict a constant temperature, while the relative humidity varies. This variation demonstrates the influence of relative humidity on weight increase. Furthermore, this approach enables comparisons with the sorption isotherm curve presented later in this subsection.

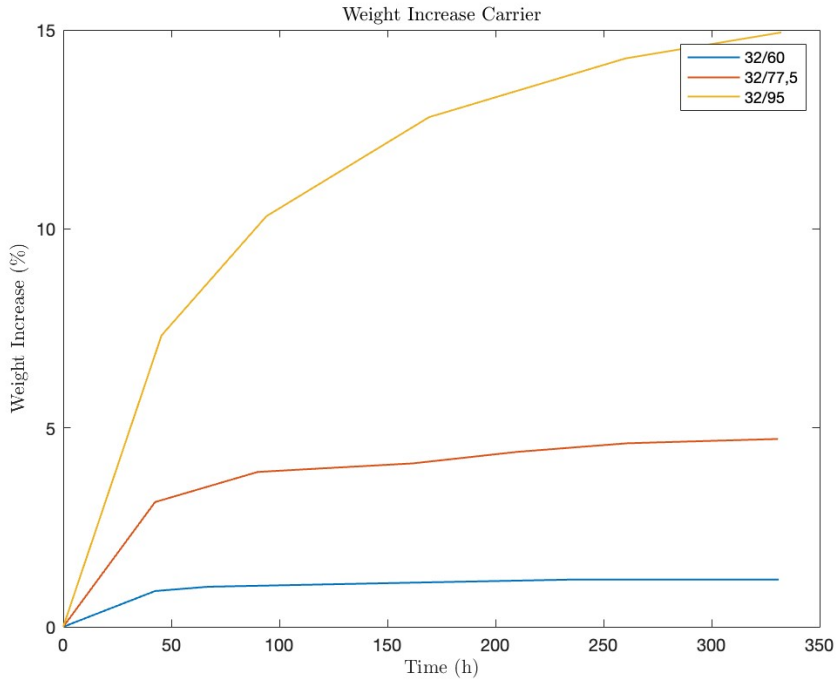

Figure 4.5: Percentage increase of carrier at 32 °C and varying relative humidity

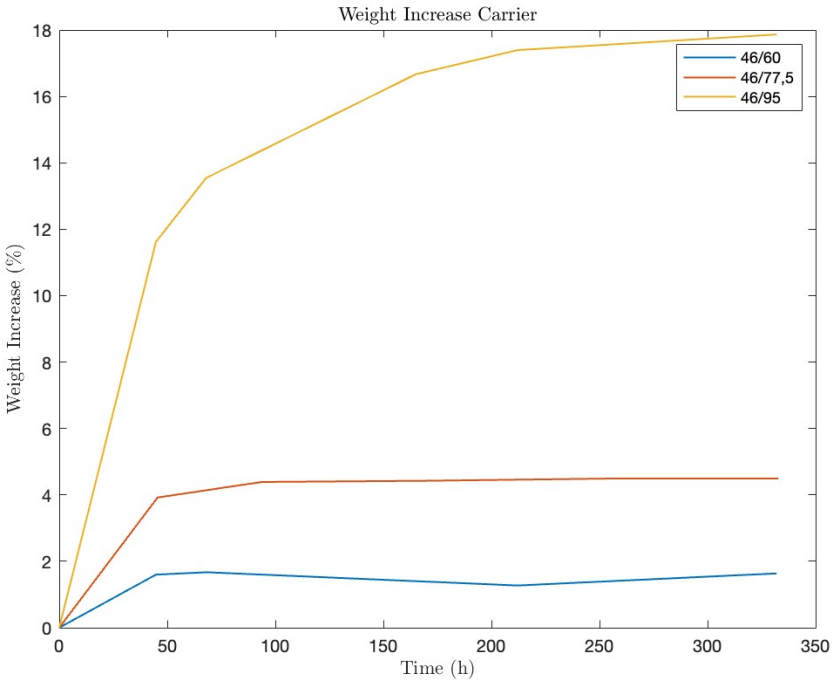

Figure 4.6: Percentage increase of carrier at 46 °C and varying relative humidity

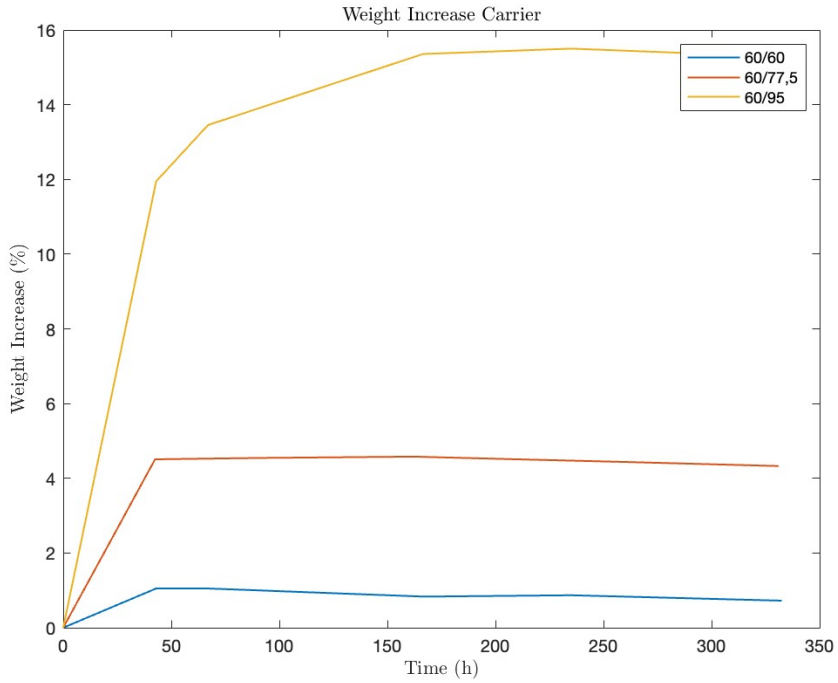

Figure 4.7: Percentage increase of carrier at 60 °C and varying relative humidity

The blue line in Figure 4.7, depicts a quite strange result. The carrier seems to be fully saturated after approximately 46 hours and is then decreasing slightly towards the end. As mentioned in the Methodology chapter, the scale had a tolerance of ± 2 g. The carrier corresponding to the blue line had a weight increase of roughly 1 %. Consequently, the scale's accuracy will significantly affect the result and fronts with lower weight increases.

The response to changes in relative humidity is non-linear despite the constant difference between the three levels. The figures above demonstrate how even small variations in higher levels of relative humidity can lead to a significant increase in carrier weight. This exponential behavior aligns with the theory of moisture absorption and the sorption isotherm curve, as discussed previously. To determine how well the measurements align with the curve in Figure 2.10, the carriers need to be

dried at 105°C, and the moisture content (w) can be calculated using Equation 2.12. The calculated moisture content can then be plotted and compared with the sorption isotherm curve for the MDF board, as illustrated in Figure 4.8.

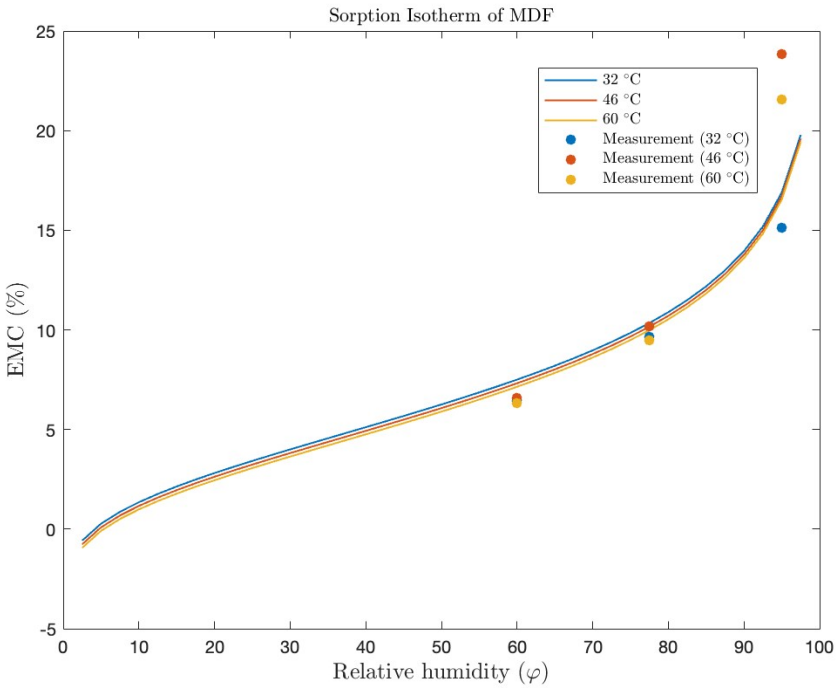

Figure 4.8: Sorption isotherm with measurements

The measurements align well with the sorption isotherm curve in the linear sections of the curve. It should however be stressed that the EMC assumes full specimen saturation. Consequently, in Figures 4.5 to 4.7, all lines should converge toward a stationary value. However, this convergence was not achieved for all tests, particularly noticeable in the deviations at 95 % relative humidity. Some curves in Figure 4.4 failed to converge, contributing to the observed discrepancies in Figure 4.8. Had all specimens been fully saturated, the sequence of measurements in Figure 4.8 would differ from the observed sequence, as lower temperatures would yield higher EMC values.

To further illustrate and summarize how weight increase responds to changes in temperature and relative humidity after approximately 330 hours, one may construct a 3D surface as depicted in Figure 4.9.

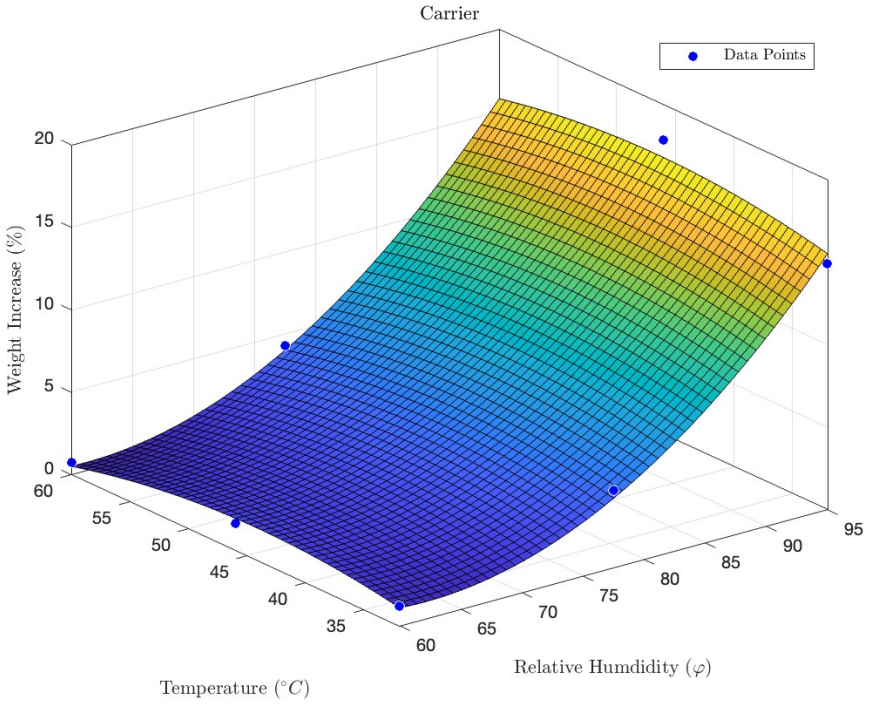

Figure 4.9: 3D surface plot for the carrier

The surface plot nicely reflects and corresponds to the previous discussion in this section, highlighting that elevated levels of relative humidity have the most significant influence on the carrier's total weight increase. Yet, it's crucial to emphasize that the data points represent the final measurements. Consequently, the surface plot does not include the effect that temperature has on the rate of weight gain in an accurate way. Instead, the derivative at any point on the surface, i.e. the slope, corresponds to the average rate of moisture absorption during the test period.

4.4 Kitchen Fronts

4.4.1 Front A

The bar chart in Figure 4.10 represents the weight increases of front A for the different tests. The blue bars indicate the fronts from the European supplier, while the red bars represent the fronts from the Asian supplier. It should be noted that the fronts from the Asian supplier were not included in all tests, as mentioned in the Methodology section. Similar to the results of the carrier, the weight increases with increasing relative humidity. However, the temperature appears to have a greater impact on the weight increase than on the uncoated carrier. This is evident when comparing the results in Figure 4.3 and 4.10 for the parameters 60/77.5 and 32/95. The uncoated carrier had a weight increase almost three times higher for 32/95 compared to 60/77.5. For front A, the corresponding tests with the same parameters showed significantly different results, where the 60/77.5 test resulted in a higher weight increase than the 32/95 test.

By comparing the results from the European and Asian supplier, one can observe that the fronts manufactured in Asia exhibit better resistance for lower relative humidities but perform worse at higher relative humidities.

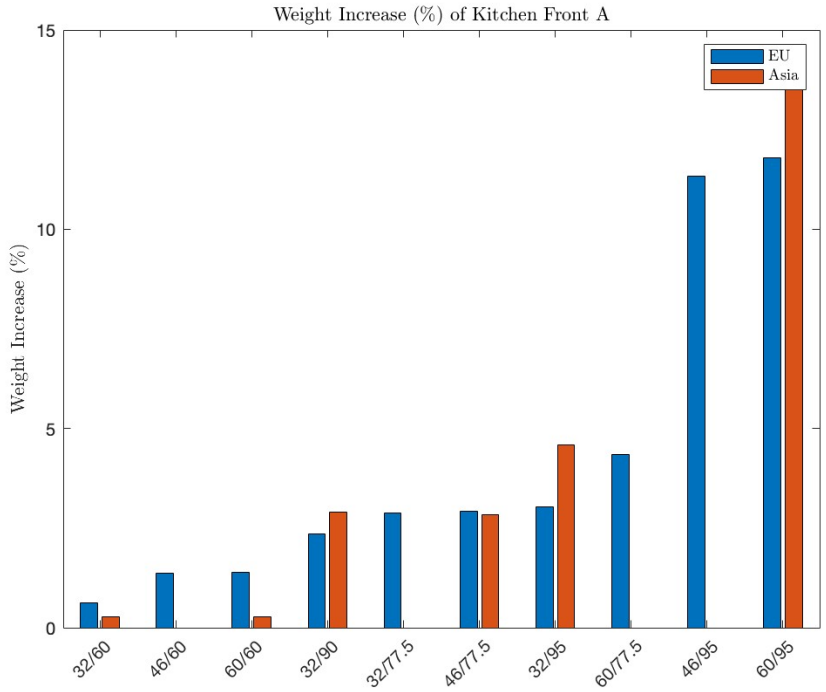

Figure 4.10: Total Weight Increase of Front A (%) after ∼330 h

The continuous weight increases during the tests can be used to demonstrate the positive correlation between temperature and weight gain. Figures 4.11 - 4.13 represent the weight increments for three tests conducted at temperatures of 32 °C, 46 °C, and 60 °C, respectively, for approximately 330 hours. The final weight increase for each test corresponds to the values shown in Figure 4.10. The rate of weight gain for the fronts exposed to a temperature of 60 °C is significantly higher than that for the fronts exposed to 32 °C, indicating that temperature increases the diffusion rate through the coating. However, all the kitchen fronts were made from similar quality MDF boards with the same density. This implies that the fronts exposed to the same relative humidity will ultimately converge towards the same value as the uncoated carrier.

The results presented in Figure 4.11 were quite unexpected. Despite the difference in relative humidity between the two tests, the yellow and purple lines almost reached the same value over the test period. This finding

contradicts the previously stated theory, which suggests that higher relative humidity should result in a greater weight increase. However, there is a clear explanation for this behavior. As shown in Table 4.1 in Section 4.2, Front A has a notably large standard deviation compared to the other fronts. In the specific tests that yielded these unexpected results, the weights of Front A deviated significantly from the mean value. For instance, the three fronts in the test with the 32/95 parameters had an average weight of 2895 g, approximately 25 g more than the mean value for all weighed fronts. Conversely, the fronts in the test with the 32/77.5 parameters had an average weight of 2815 g, about 55 g less than the overall mean value. This resulted in a difference of approximately 80 g between these specific tests. It is possible that the fronts that weighed more than the mean had a slightly thicker layer of coating, while the others had a slightly thinner layer. This variation in coating thickness could account for the observed behavior, explaining why the expected correlation between relative humidity and weight increase was not evident in these tests.

As discussed previously, the fronts from the Asian supplier performed better than the fronts from the European supplier in the test with a relative humidity of 60 %, and worse in the test with a relative humidity of 95 %. This is represented in Figure 4.11 below. Another notable observation from the tests at 32 °C is that they increased almost linearly throughout the whole test frame, indicating that they are far from being saturated.

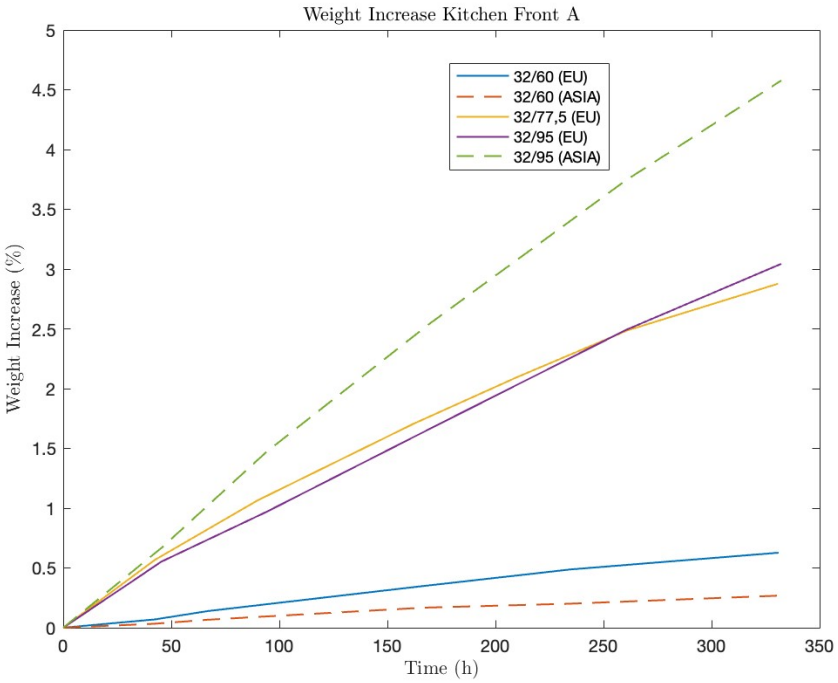

Figure 4.11: Percentage increase of front A at 32 °C and varying relative humidity

Figure 4.12 below depicts the tests conducted at 46 °C. For the test with the intermediate levels of both temperature and relative humidity, 46/77.5, the results from the two suppliers are almost identical.

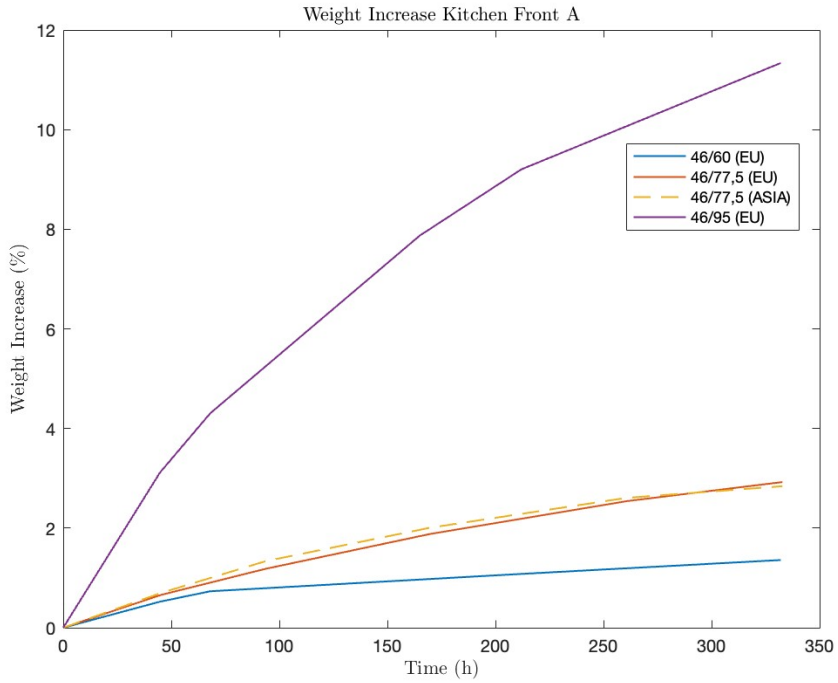

Figure 4.12: Percentage increase of front A at 46 °C and varying relative humidity

Similar to the test results at 32 °C, it appears that the fronts from the Asian supplier perform better in low humidity conditions, but worse in high humidity conditions compared to those from Europe. This can be observed in Figure 4.13 which presents the test results at 60 °C. It is interesting to note that the tests conducted at high temperatures and low relative humidity converge quite rapidly. As explained previously in the theory, this is because higher temperatures increase the water vapor diffusion rate. Moreover, lower ambient relative humidity reduces the EMC of the MDF board.

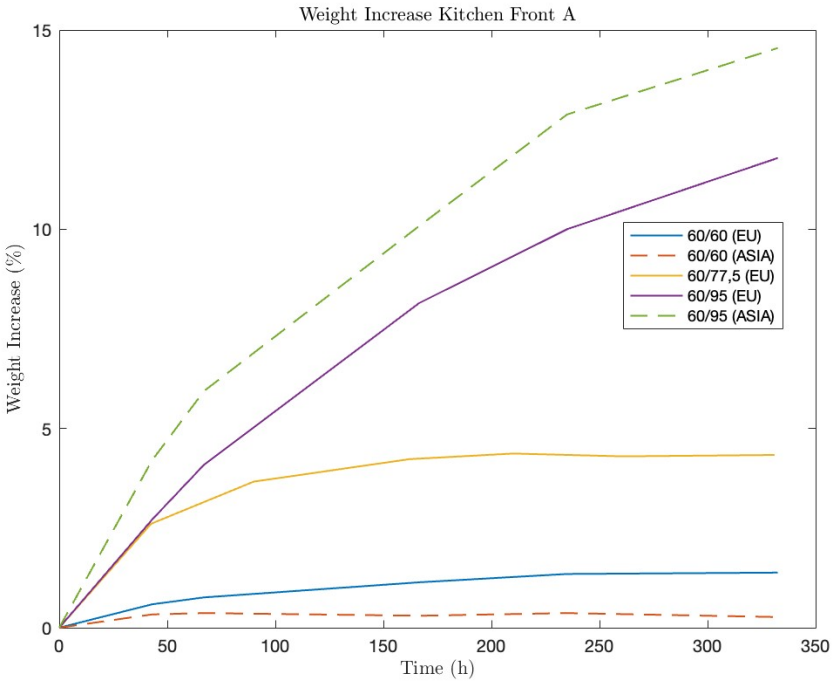

Figure 4.13: Percentage increase of front A at 60 °C and varying relative humidity

Figures 4.14a and 4.14b show a 3D surface that represents the weight increment after approximately 330 hours for the respective tests. A combination of high relative humidity and high temperature leads to the highest weight increase. Temperature alone does not seem to have a significant impact on the weight increase, but relative humidity does.

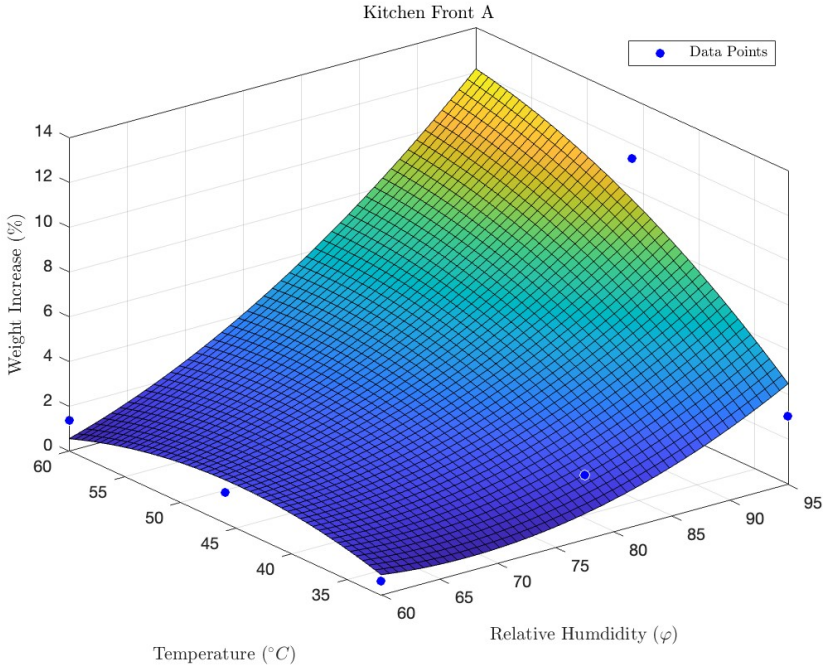

(a) European Supplier

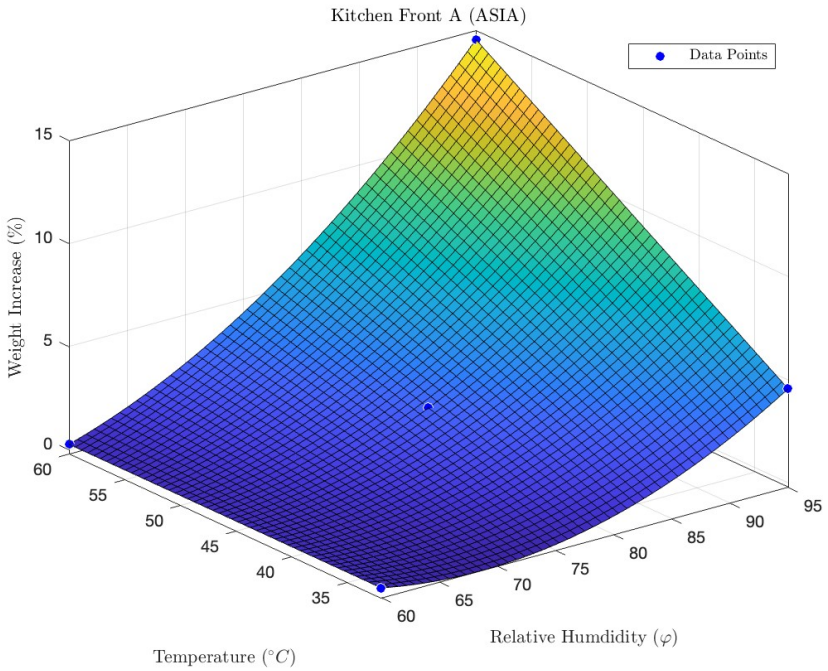

(b) Asian Supplier

Figure 4.14: 3D surface for front A

4.4.1.1 Comparison with Implemented Parameters

As previously mentioned, conducting tests is a time-consuming task. Thus, it is desirable to minimize the test period while still ensuring accurate results. Since the moisture absorption rate depends on the moisture gradient between the test sample and the surrounding air, implementing more aggressive parameters of temperature and relative humidity can accelerate the process. Figure 4.15 compares the currently implemented parameters at IKEA, i.e., 32/90, with the most extreme temperature and relative humidity levels selected during this project. This comparison demonstrates that the total amount of moisture absorbed during the test period with the current parameters could be achieved in a significantly shorter time by using higher levels of temperature and relative humidity. Consequently, considering weight increase as the only response variable of interest, the required time could be reduced from approximately 330 hours to around 30 and 37 hours for Asian- and European-produced fronts, respectively.

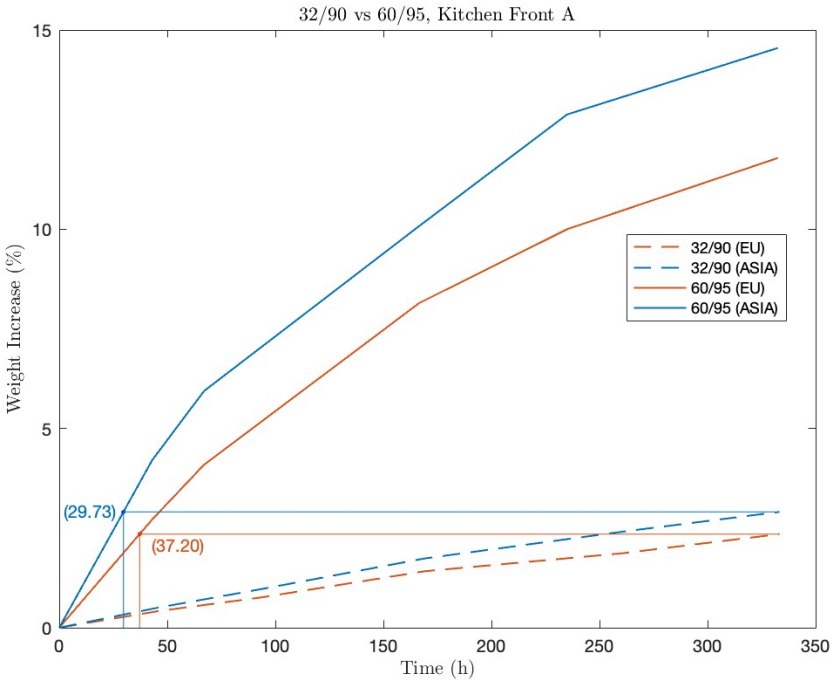

Figure 4.15: Comparison between 32/90 and 60/95

4.4.1.2 Defects on Front A

Figure 4.16a and 4.16b demonstrate how cracks emerge in the longitudinal direction of the board during elevated levels of temperature and relative humidity. This behavior is caused by the coating not being able to withstand the moisture-induced movement of the carrier. The direction of the cracks aligns with the theory regarding the expansion of MDF, which states that the movement caused by moisture absorption and desorption will predominantly be in the thickness direction due to the orientation of the fibers. When comparing Figure 4.16a and 4.16b, it is noticeable that there are more cracks on the front from the Asian supplier. This observation is consistent with Figure 4.10, which indicates a greater increase in weight for the front from the Asian supplier.

(a) European Supplier (60/95)

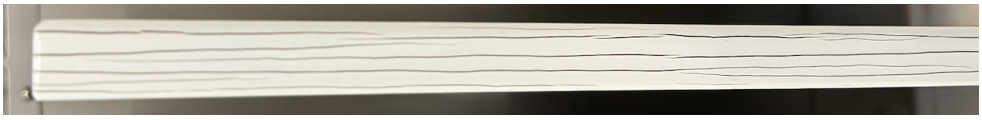

(b) Asian Supplier (60/95)

Figure 4.16: Crack formation on Front A

Another defect that can result from the absorption of moisture into the wood is fiber raising. This visual defect is caused by the expansion of fibers on the surface of the MDF board, resulting in a texture similar to orange peel. Figure 4.17 shows a surface without and with fiber raising, respectively.

Figure 4.17: Fiber raising front A (60/95)

4.4.2 Front B

In general, the findings indicate that front B closely resembles front A in most aspects. However, one discrepancy between the results is that front B consistently exhibited slightly less weight gain than front A. This

variation could be attributed to the slightly higher density of front B, necessary to achieve optimal surface quality after the milling operation. Additionally, front B has a greater thickness than front A, which impacts the diffusion rate to saturation.

The weight increase results for front B are depicted in Figure 4.18. Similar to front A, the fronts from the Asian supplier exhibited greater sensitivity to higher levels of humidity. However, this test reveals an even larger disparity between the two suppliers. While the fronts from the Asian supplier performed better at lower levels of humidity, those from the European supplier demonstrated greater resistance at higher humidity levels. As observed with front A, temperature had a significant impact on the weight increase, and the combination with high humidity accelerated the rate of weight increase significantly.

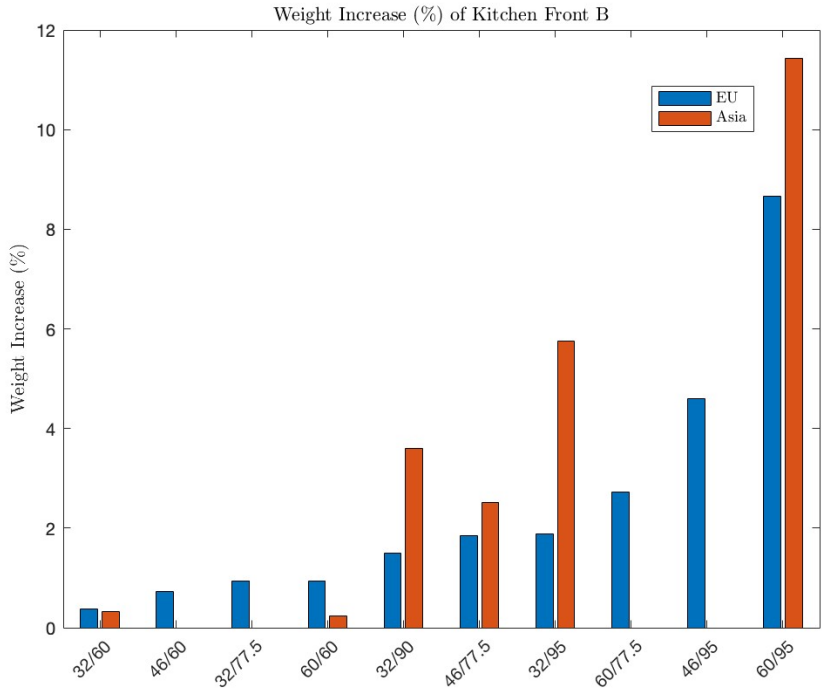

Figure 4.18: Total weight increase of front B (%) after ∼330 h

The graph presented in Figure 4.19 - 4.21 displays the increase in weight

throughout the approximately 330-hour testing period. One noteworthy observation is the difference in weight gain rate between the fronts from the Asian and European suppliers in the 32/95 parameter test, where the fronts from the Asian supplier exhibited an almost three times larger increase compared to the ones from Europe.

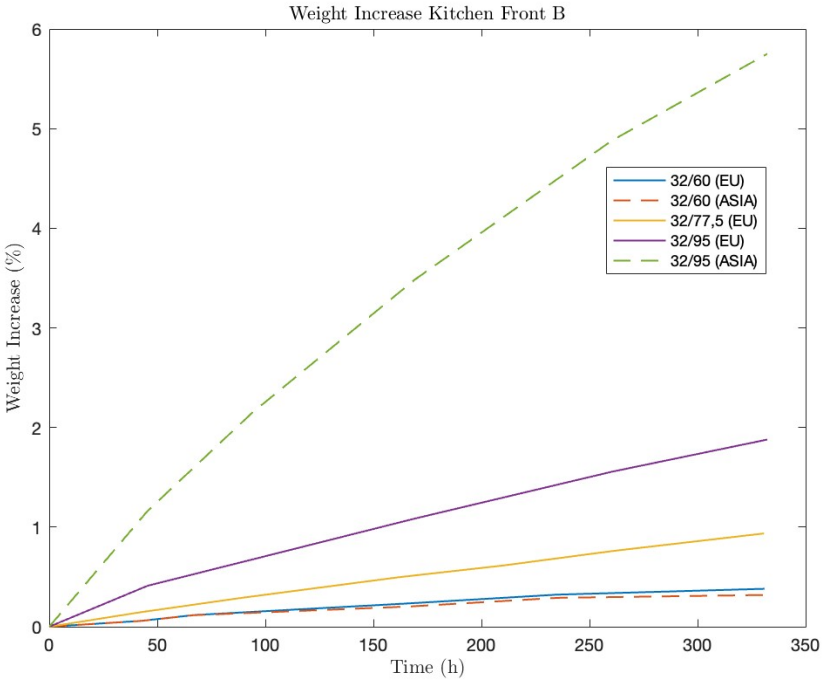

Figure 4.19: Percentage increase of front B at 32 °C and varying relative humidity

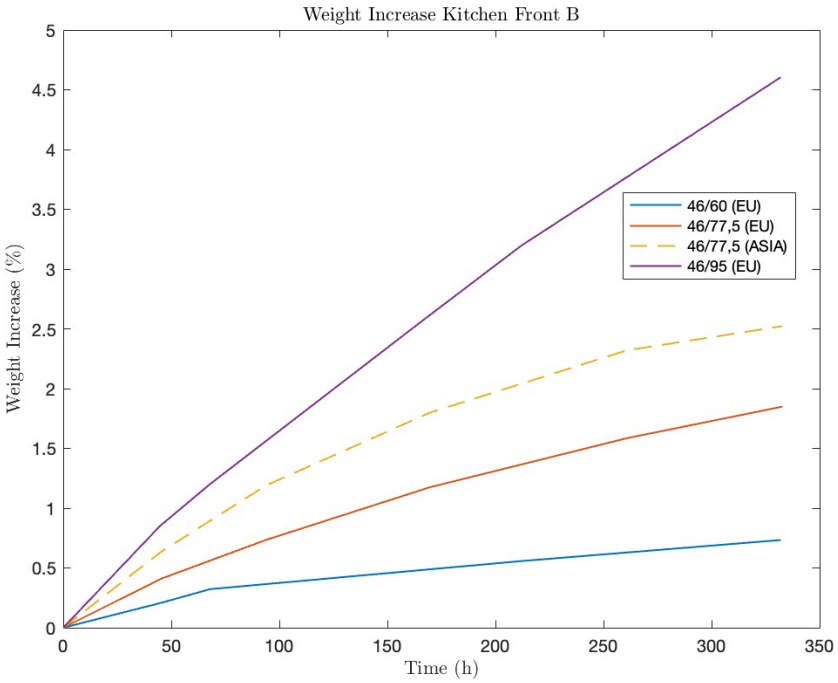

Figure 4.20: Percentage increase of front B at 46 °C and varying relative humidity

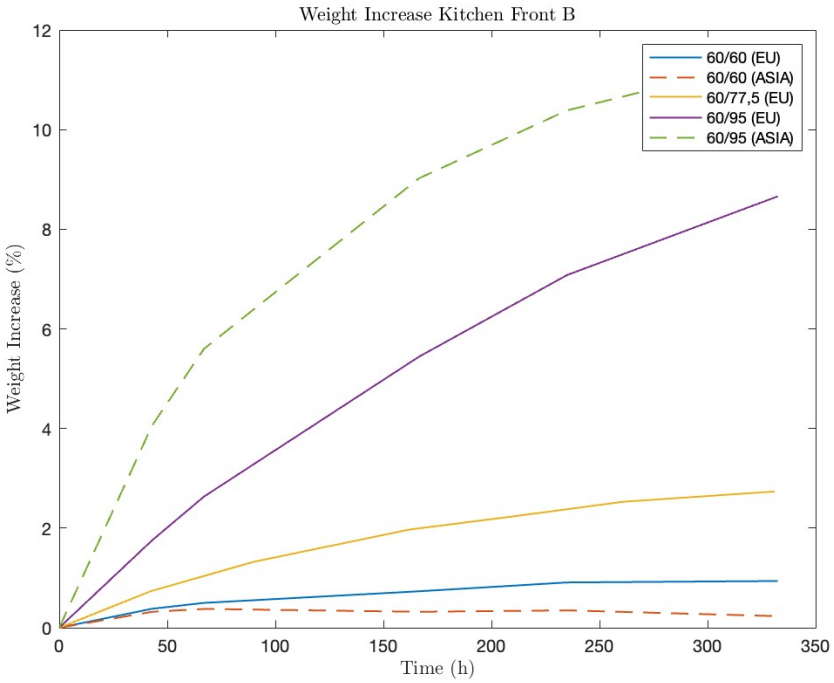

Figure 4.21: Percentage increase of front B at 60 °C and varying relative humidity

The 3D surface plot in figure 4.22a clearly shows that the simultaneous increase in temperature and humidity results in a noticeable increase in weight increase. The same goes for the fronts from Asia which are represented in figure 4.22b. However, a high level of humidity and low temperature results in a higher weight increase than for the ones from Europe.

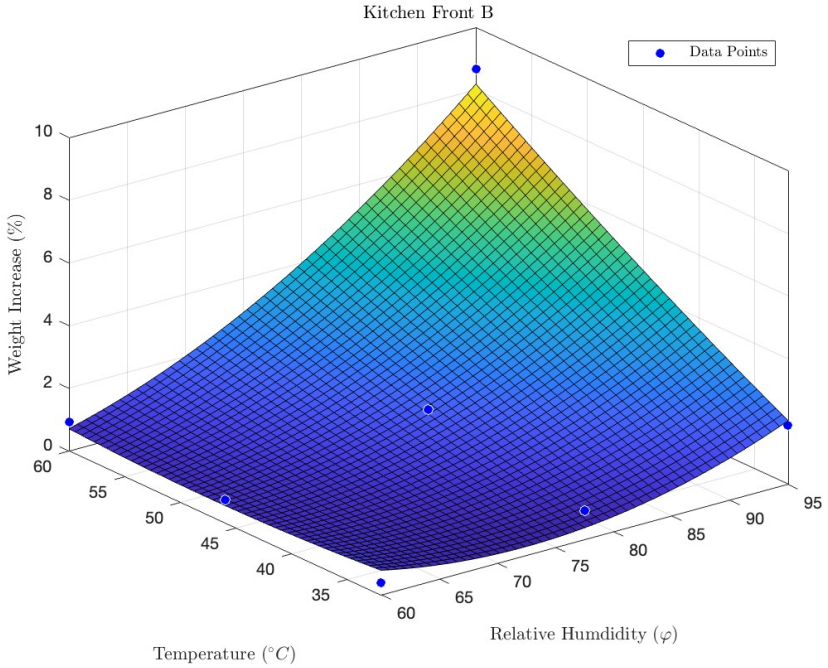

(a) European Supplier

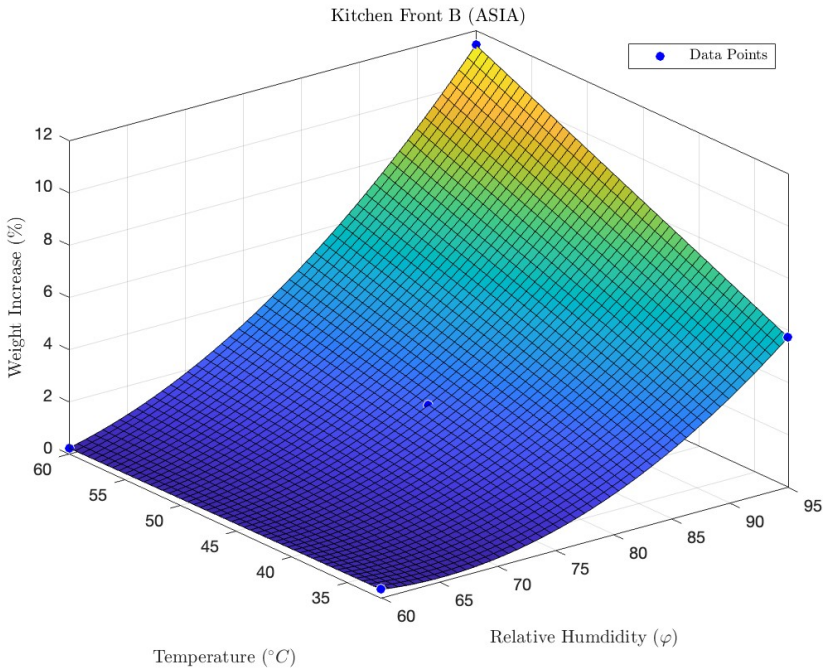

(b) Asian Supplier

Figure 4.22: 3D surface for front B

4.4.2.1 Comparison with Implemented Parameters

The current testing parameters, 32/90, yield a weight increase of 1.49 % and 3.6 % for the European and Asian front B suppliers, respectively. This weight increase could be attained in approximately 37 and 38 hours by elevating the parameters to 60/95. Figure 4.23 below illustrates the comparison between the testing parameters.

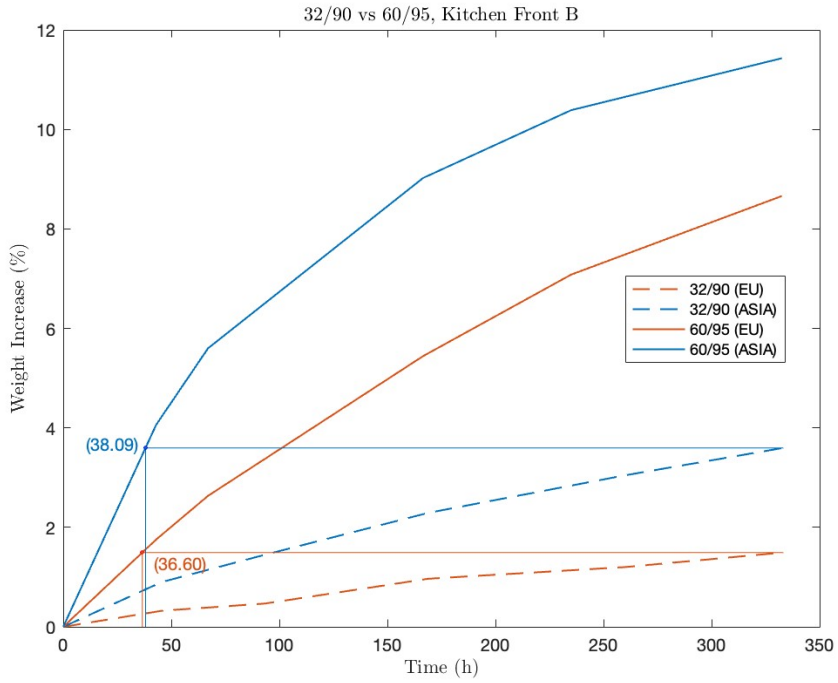

Figure 4.23: Comparison between 32/90 and 60/95

4.4.2.2 Defects on Front B

During the test series, no crack formation was found on front B. However, similar to the defects of front A, fiber raising was present, especially in tests with the largest weight gain (60/95), see Figure 4.24a. Figure 4.24b represents front B before testing.

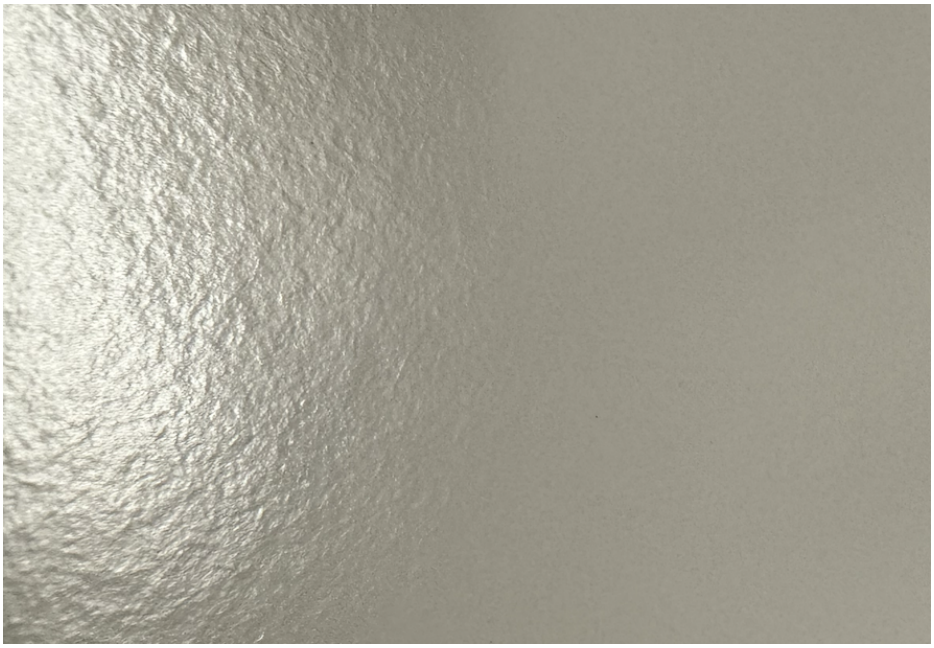

(a) With fiber raising (60/95)

(b) Without fiber raising

Figure 4.24: Front B with and without fiber raising

4.5 Factorial Design

An interaction plot can be generated for the different levels of the 2^2 and 3^2 factorial analysis to demonstrate how variations in temperature and relative humidity of the surrounding air affect the weight of both coated and uncoated carriers. These interactions will be separately presented for the carrier and each kitchen front. Furthermore, each section will include an analysis of variance (ANOVA) to assess the statistical significance of the gathered data.

4.5.1 Carrier

As stated in Section 2.3.1, the different levels of temperature and relative humidity are indicated as -1, 0, and 1, respectively. Keeping the relative humidity at a constant level while the temperature varies between -1 and 1 allows for an overview of how the weight increase is affected by different levels of the two factors, as depicted in Figure 4.25.

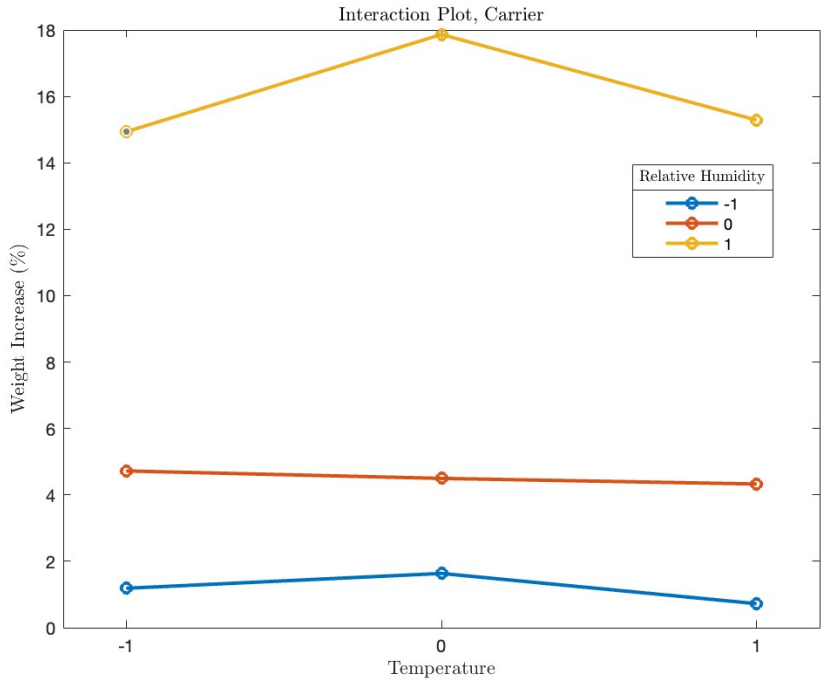

Figure 4.25: Interaction between temperature and relative humidity for the carrier

As depicted in Figure 4.25, the lines appear largely parallel, indicating a negligible interaction effect between the factors. However, there exists a positive correlation between the dependent variable, weight increase, and the relative humidity of the surrounding air, consistent with the observations and discussions in Section 4.3. This is highlighted by the significant vertical gap between the lines. It is important to note that these plots are based on the weight increase after 330 hours, which did not always allow for complete convergence towards the stationary value of the EMC. Had the test period allowed for full saturation of the tested carriers, the slope of all three lines in Figure 4.25 would have been negative, as higher temperatures lead to lower levels of EMC and consequently lower weight increase.

4.5.1.1 Analysis of Variance

ANOVA analysis is crucial in this context for providing statistical validation for the observed trends and relationships depicted in Figure 4.25. The result from this analysis is compiled and presented in Table 4.3.

Table 4.3: ANOVA Table

Source of Variation	Df	Sum Sq	Mean Sq	F value	*Pr(>F)*	
Temperature	2	5504	2752	37.76	3.63×10^{-7}	***
Humidity	2	837019	418509	5741.75	$< 2 \times 10^{-16}$	***
Temperature:Humidity	4	6267	1567	21.50	1.18×10^{-6}	***
Residuals	18	1312	73			

Signif. codes: 0 '***' 0.001 '**' 0.01 '*' 0.05 '.' 0.1 ' ' 1

Firstly, it should be noted that all factors that impact the dependent variable are statistically significant. However, just as depicted in Figure 4.25, relative humidity is the dominant factor that impacts the weight increase as indicated by the large F value.

4.5.2 Kitchen Front A

In this section, the interaction plot for both the Asian and European suppliers will be presented. However, since no tests were conducted at an intermediate level, the interaction plot for the Asian supplier will only include low and high levels of each factor, denoted as 0 and 1.

The impact and relationship between the dependent and independent factors show different behavior compared to the carrier. When examining Figure 4.26, a significant increase in the slope of the curves can be observed, indicating that temperature has a greater influence. This behavior is expected because the coating of the carrier tends to change its resistance to moisture diffusion as the temperature increases. The unexpected result in the weight increment for the tests representing the low level of temperature for the red and yellow line is explained earlier in the Result and Discussion section. This could be derived from the deviating coating thickness of the kitchen fronts.

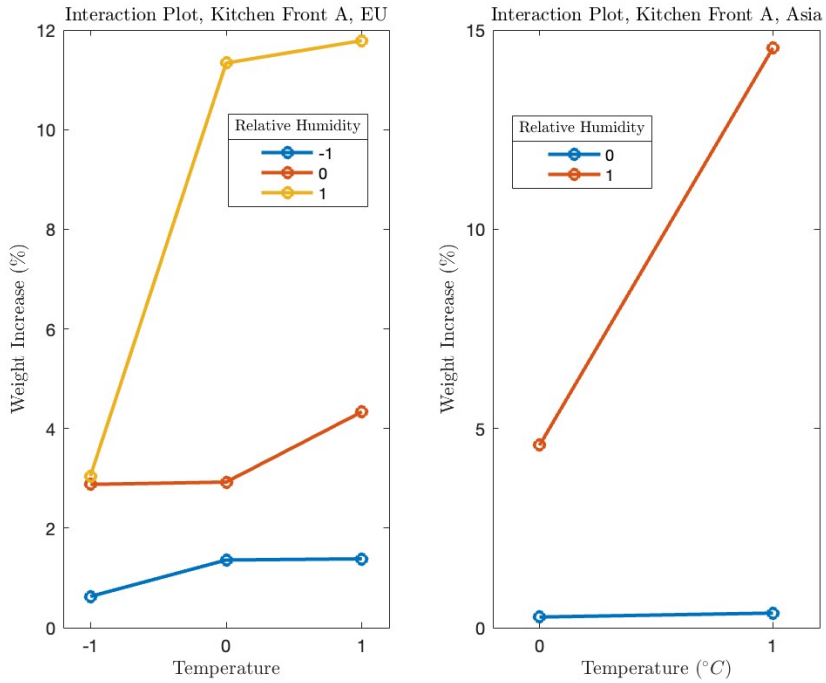

Figure 4.26: Interaction between temperature and relative humidity

4.5.2.1 Analysis of Variance

From Table 4.4 and 4.5, it can be observed that the difference in impact between temperature and humidity has decreased, as indicated by the smaller difference in the F value. This aligns well with the plots depicted in Figure 4.26, where the slope of the curves indicates a positive correlation between temperature and weight increase.

Table 4.4: ANOVA Table (EU)

Source of Variation	Df	Sum Sq	Mean Sq	F value	*Pr(>F)*	
Temperature	2	57530	28765	41.04	1.97×10^{-7}	***
Humidity	2	227742	113871	162.47	3.02×10^{-12}	***
Temperature:Humidity	4	68225	17056	24.34	4.72×10^{-7}	***
Residuals	18	12616	701			

Signif. codes: 0 '***' 0.001 '**' 0.01 '*' 0.05 '.' 0.1 ' ' 1

Table 4.5: ANOVA Table (ASIA)

Source of Variation	Df	Sum Sq	Mean Sq	F value	*Pr(>F)*	
Temperature	1	66901	66901	205.4	5.48×10^{-7}	***
Humidity	1	231852	231852	711.9	4.19×10^{-9}	***
Temperature:Humidity	1	67500	67500	207.3	5.30×10^{-7}	***
Residuals	8	2605	326			

Signif. codes: 0 '***' 0.001 '**' 0.01 '*' 0.05 '.' 0.1 ' ' 1

4.5.3 Kitchen Front B

Figure 4.27 illustrates a positive correlation between temperature and weight gain, particularly evident at higher relative humidity levels, as indicated by the steepening slope of the curves. Notably, the weight gain for the European supplier exhibits an exponential trend with rising temperature and relative humidity. A conclusion regarding similar behavior for the Asian supplier cannot be made, since only two levels of each factor are present.

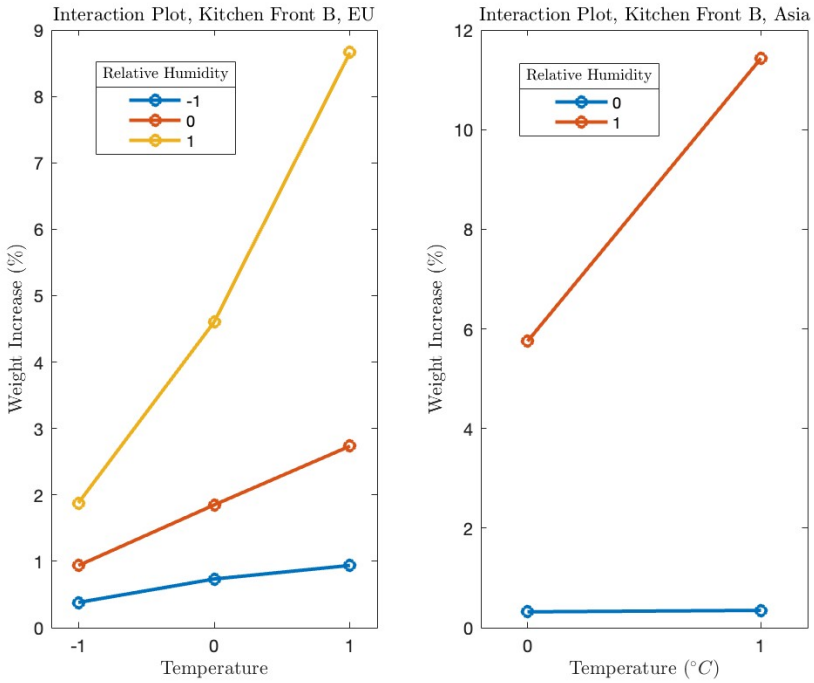

Figure 4.27: Interaction between temperature and relative humidity

4.5.3.1 Analysis of Variance

Similar to the discussion in Subsection 4.5.2.1, when comparing Table 4.6 and 4.7, it is evident that the difference in the impact of temperature and humidity has decreased, as shown by the reduced gap in the F values. Just as for the previously presented Anova tables above, the results are statistically significant.

Table 4.6: ANOVA Table (EU)

Source of Variation	Df	Sum Sq	Mean Sq	F value	*Pr(>F)*	
Temperature	2	48740	24370	191.72	7.33×10^{-13}	***
Humidity	2	107152	53576	421.49	7.63×10^{-16}	***
Temperature:Humidity	4	38833	9708	76.38	4.85×10^{-11}	***
Residuals	18	2288	127			

Signif. codes: 0 '***' 0.001 '**' 0.01 '*' 0.05 '.' 0.1 ' ' 1

Table 4.7: ANOVA Table (ASIA)

Source of Variation	Df	Sum Sq	Mean Sq	F value	*Pr(>F)*	
Temperature	1	28227	28227	3682	6.05×10^{-12}	***
Humidity	1	245960	245960	32082	1.06×10^{-15}	***
Temperature:Humidity	1	29800	29800	3887	4.87×10^{-12}	***
Residuals	8	61	8			

Signif. codes: 0 '***' 0.001 '**' 0.01 '*' 0.05 '.' 0.1 ' ' 1

4.6 Sources of Error

When conducting the experiment, several sources of errors were identified that may have impacted the result. It is crucial to understand these sources to interpret the findings accurately and to minimize similar errors in future research.

One potential source of error was the initial weight discrepancies. Some kitchen fronts had initial weights that deviated from the overall average weight of all the samples. As discussed earlier, the deviation between two tests of front A, was as much as 80 g in one case. This could have influenced the results, as the rate of water absorption may differ based on the initial weight. The difference in weight between the fronts can be due to several factors including variations in dimensions, coating thickness, MDF density, etc.

As mentioned earlier, the scale used in the experiment had an accuracy of $\pm$ 2 g. For tests where the weight gain of the kitchen fronts was relatively low, the margin of error introduced by the scale could represent a substantial proportion of the observed weight gain, thereby affecting the reliability of the data. However, in the majority of the tests, the weight increase from start to finish was sufficiently large to not be significantly affected by the precision of the scale.

For the experiments, three different climate chambers were utilized. Two of the chambers were of the same model, while the third was a slightly different model. The chambers were not calibrated simultaneously, so

there is a possibility that they may differ somewhat from each other in terms of accuracy.

Figure A.2 illustrates that the humidity level in the climate chamber for the specific test decreased before a weighing session. This was not noticed until the test was completed and the data were extracted. That meant that the kitchen fronts in the climate chamber could have lost some weight before the weighing since the humidity level was decreased from 77,5 % to approximately 70 %. This is slightly evident in the result for the carrier in Figure 4.5 where one can see that the red curve has a strange appearance. The gradient decreases slightly between hours 90 and 170, then increases again, a behavior that should not be possible. There were no unusual behaviors observed for front A and B, likely because the coating delayed the release of moisture, preventing it from affecting the measurements. It is also important to note that the overall weight increase during the entire testing period was not impacted, likely due to the relatively short period of reduced humidity.

Just as the kitchen fronts absorb moisture, they also release moisture due to desorption. To minimize the impact of moisture desorption, it was important to weigh the fronts quickly after removing them from the climate chambers. This was especially crucial for the carriers as they lacked any coating to reduce the rate of moisture desorption. Despite efforts to weigh them promptly, there may have been some variations in the recorded weights due to ongoing moisture desorption.

Chapter 5

Conclusions and Future Work

5.1 Conclusions

The primary aim of this study was to investigate and analyze the impact of humidity on kitchen fronts, intending to gain a comprehensive understanding of this relationship. Additionally, the study aimed to explore the potential for shortening the required testing period in climate chambers by further accelerating the testing process. The effects of relative humidity and temperature on the response variable, water sorption, were examined using the design of experiments (DoE) methodology. The study focused on two different families of coated kitchen fronts and one uncoated front. The two coated fronts, labeled A and B, are manufactured in both Europe and Asia and the tests included samples from both suppliers for each type of front.

The study revealed that the level of relative humidity predominantly determines the water sorption gain over time, while the temperature level controls the rate of water sorption. This finding aligns with the presented theory that the equilibrium moisture content (EMC) is primarily determined by relative humidity. The theory also indicates that the water vapor permeability constant δ_v, with regards to water diffusion in wood, depends on temperature. Furthermore, the study showed that temperature has a significantly larger impact on the coated kitchen fronts compared to the uncoated ones. This observation supports the

theory that temperature positively correlates with water permeability through the coating.

This study emphasizes the importance of conducting tests during the product development phase. By performing accelerated tests and adjusting parameters such as relative humidity and temperature, developers can significantly reduce test durations by up to 90 %. This reduction in testing time leads to shorter development cycles and lower costs. Accelerated testing allows for quicker iterations in the design process, providing faster feedback on material performance and product reliability. As a result, it enables more efficient product development and shorter lead times to market and customers.

5.2 Recommendation for Future Work

In this study, the temperature and relative humidity remained constant throughout each test. However, in reality, these factors fluctuate over time, as evidenced in Figure 1.2 in the Introduction chapter. Over extended periods, these fluctuations can cause the carrier to both lose and gain weight depending on the relative humidity of the surrounding air, leading to moisture-induced movements that may result in coating fatigue. Since the climate chambers allow for cycling of both temperature and humidity, this investigation may provide valuable insights into how the carrier will behave in customers' homes. Nevertheless, if such tests are to be conducted, a scale that allows for continuous monitoring of the carriers' weight over time should be used, particularly since they will experience weight fluctuations, and thus data on the weight must be collected more frequently.

Even though hourly peaks above 90 % relative humidity may occur, it is not critical to design for these brief spikes. If the surfaces have no damage to the coating, they will not immediately respond to sudden increases in relative humidity due to the delay in the diffusion process caused by the coating. However, several consecutive days of high relative humidity are more harmful, and the surfaces should be designed to withstand such

prolonged exposure.

Additionally, it is recommended to create a sorption isotherm curve for the MDF carrier by conducting several tests where the temperature remains constant while the relative humidity varies. During these tests, all MDF carriers must be fully saturated. Thus, plotting the weight increase over time is recommended to observe if the graph has converged, indicating saturation of the carrier. After each test, the carrier needs to be dried since the EMC requires the specimen to have a dry weight. Since the coated fronts will converge towards the same stationary value as the carrier, the sorption isotherm curve may be used as a guideline to determine how much moisture the fronts will gain depending on the geographical location of the final customer.

Bibliography

[1] IKEA, "Internal Documents and Data."

[2] C.-H. Lo, "Application of Refined Kano's Model to Shoe Production and Consumer Satisfaction Assessment," *Sustainability*, vol. 13, no. 5, p. 2484, Jan. 2021, number: 5 Publisher: Multidisciplinary Digital Publishing Institute. [Online]. Available: https://www.mdpi.com/2071-1050/13/5/2484

[3] D. C. Montgomery, *Design and analysis of experiments*, eighth edition ed. Hoboken, NJ: John Wiley & Sons, Inc, 2013.

[4] "World first: Unilin is the first company to recycle MDF." [Online]. Available: https://www.unilinpanels.com/en/about-unilin-panels/sustainability/circularity/recycled-mdf-hdf

[5] "Medium Density Fiberboard (MDF) - Home Pillars," Dec. 2020. [Online]. Available: https://homepillars.com/product/raw-panels/medium-density-fiberboard-mdf,https://homepillars.com/product/raw-panels/medium-density-fiberboard-mdf

[6] "HMR Particle Board." [Online]. Available: https://www.bord.com.au/products/hmr-particleboard

[7] T. Walther, H. Thömen, T. Donath, and F. Beckmann, "Microstructure of Medium Density Fiberboard (MDF)," *DESY*, 2004. [Online]. Available: https://hasyweb.desy.de/science/annual_reports/2004_report/part1/contrib/41/12060.pdf

[8] "Understanding psychrometric charts and dew points | Angelica Isa." [Online]. Available: https://angelicaisa.com/blog/understanding-dewpoint

[9] J. Shi and S. Avramidis, "Evolution of wood cell wall nanopore size distribution in the hygroscopic range," *Holzforschung*, vol. 73, no. 10, pp. 899–910, Oct. 2019, publisher: De Gruyter. [Online]. Available: https://www.degruyter.com/document/doi/10.1515/hf-2018-0198/html

[10] K. Sandin, *INTRODUKTION TILL FUKTMEKANIKEN*, ser. Fuktsäkerhet i byggnader. Formas, 2001.

[11] IKEA Museum, "The road from trading pens to furniture - IKEA Museum," 2024. [Online]. Available: https://ikeamuseum.com/en/explore/the-story-of-ikea/the-birth-of-ikea/

[12] IKEA, "The IKEA vision, values and business idea," 2024. [Online]. Available: https://www.ikea.com/gb/en/this-is-ikea/about-us/the-ikea-vision-and-values-pub9aa779d0

[13] "How we work – IKEA Global." [Online]. Available: https://www.ikea.com/global/en/our-business/how-we-work/

[14] IKEA, "Kitchen - 25 Year Limited Warranty INCLUDED." [Online]. Available: https://www.ikea.com/us/en/files/pdf/b4/41/b441e26c/sektion_warranty_a5-1.pdf

[15] I. Gremyr, B. Bergquist, and M. Elg, *Quality Management - An introduction*, 1st ed. Studentlitteratur, 2020.

[16] L. Sandholm, *Total Quality Management*, 2nd ed. Lund: Studentlitteratur, 2000.

[17] SIS - Svenska Insitutet för Standarder, "Ledningssystem för kvalitet - Krav (ISO 9001:2015)," 2015. [Online]. Available: https://www-sis-se.ludwig.lub.lu.se/api/document/get/8016642

[18] Necip Doganaksoy, William Q. Meeker, and Gerald J. Hahn, *Achieving Product Reliability: A Key to Business Success.* New York: Chapman and Hall/CRC, Jun. 2021.

[19] W. Nelson, *Accelerated testing: statistical models, test plans and data analyses*, ser. Wiley series in probability and mathematical statistics. New York: Wiley, 1990.

[20] L. Escobar and W. Meeker, "A Review of Accelerated Test Models," *Statistical Science*, vol. 21, Sep. 2007.

[21] H.-C. Liu, L. Liu, and N. Liu, "Risk evaluation approaches in failure mode and effects analysis: A literature review," *Expert Systems with Applications*, vol. 40, no. 2, pp. 828–838, Feb. 2013. [Online]. Available: https://www.sciencedirect.com/science/article/pii/S0957417412009712

[22] S. G. Rabinovich, *Measurement errors and uncertainties: theory and practice*, 3rd ed. New York, NY: AIP Press, Springer, 2005.

[23] P. G. Burström, *Byggnadsmaterial - Tillverkning, egenskaper och användning*. Studentlitteratur, 2021, vol. 4.

[24] P. Niemz, A. Teischinger, and D. Sandberg, Eds., *Springer handbook of wood science and technology*, ser. Springer handbooks. Cham: Springer, 2023.

[25] P. Kibleur, Z. Manigrasso, W. Goethals, J. Aelterman, M. N. Boone, J. Van Acker, and J. Van den Bulcke, "Microscopic deformations in MDF swelling: a unique 4D-CT characterization," *Materials and Structures*, vol. 55, no. 7, p. 206, Sep. 2022. [Online]. Available: https://doi.org/10.1617/s11527-022-02044-1

[26] L. E. Nevander and B. Elmarsson, *FUKT - Handbok*, 3rd ed. Svensk Byggtjänst, 2006.

[27] N. S. Nandagopal, *Fluid and thermal sciences: a practical approach for students and professionals*. Cham: Springer, 2022.

[28] F. A. Kulacki, Ed., *Handbook of thermal science and engineering*, ser. Springer reference. Cham: Springer, 2018.

[29] T. Gereke, "Moisture-induced stresses in cross-laminated wood panels," *ETH Zürich*, 2009. [Online]. Available: https://www.research-collection.ethz.ch/bitstream/handle/20.500.11850/151409/eth-201-02.pdf

[30] Q. Wu, "Application of Nelson's Sorption Isotherm to Wood Composites and Overlays," *Wood and Fiber Science*, pp. 187–191, 1999. [Online]. Available: https://wfs.swst.org/index.php/wfs/article/view/860

[31] S. Avramidis and J. F. Siau, "An investigation of the external and internal resistance to moisture diffusion in wood," *Wood Science and Technology*, vol. 21, no. 3, pp. 249–256, Sep. 1987. [Online]. Available: https://doi.org/10.1007/BF00351396

[32] J. Graystone, "Moisture transport through wood coatings: The unanswered questions," *Surface Coatings International Part B: Coatings Transactions*, vol. 84, no. 3, pp. 177–187, Jul. 2001. [Online]. Available: https://doi.org/10.1007/BF02700396

Appendix A

Temperature Log From the Climate Chamber

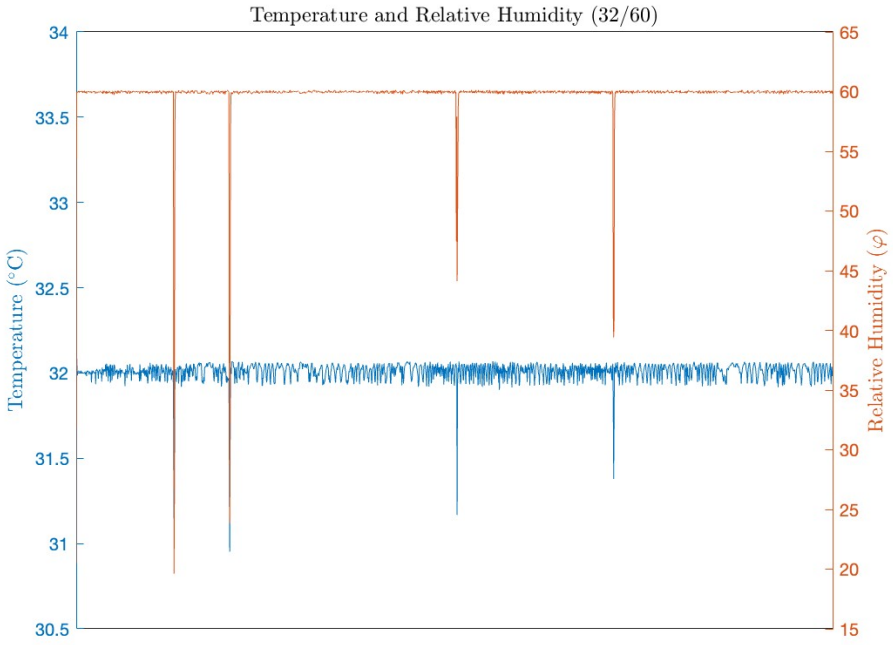

Figure A.1: Temperature = 32 °C, $\varphi = 60$

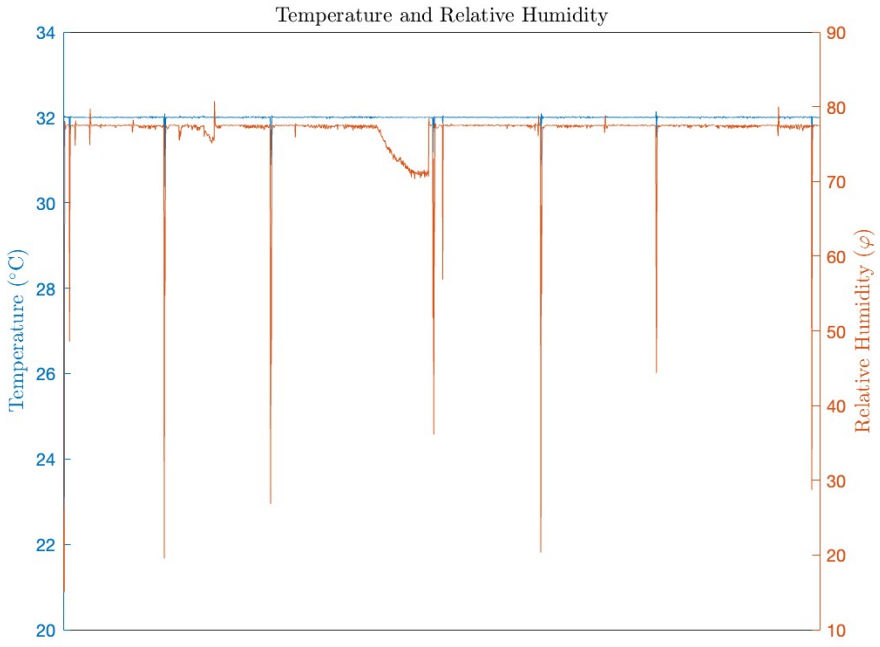

Figure A.2: Temperature = 32 °C, $\varphi = 77.5$

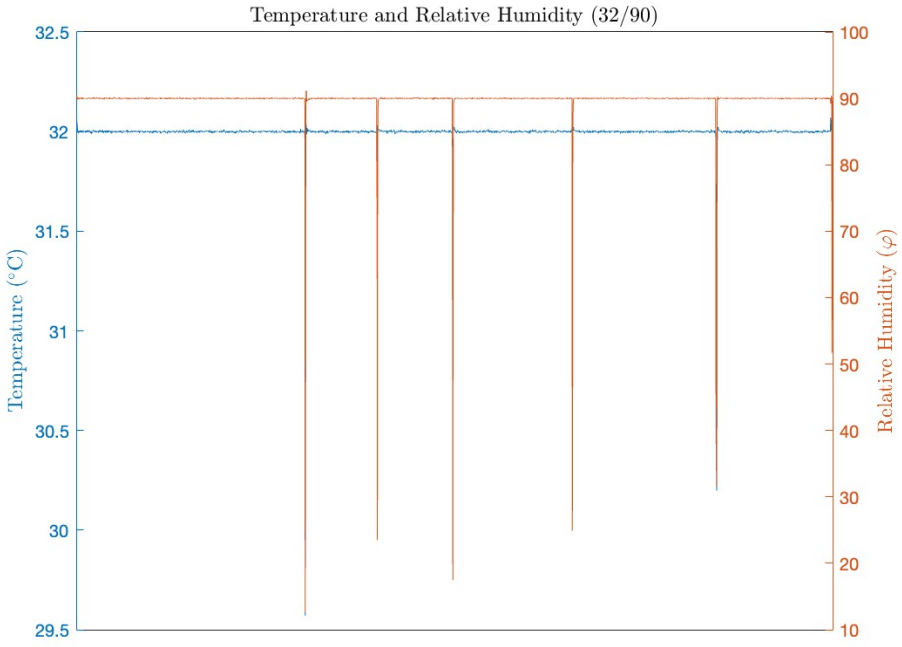

Figure A.3: Temperature = 32 °C, $\varphi = 90$

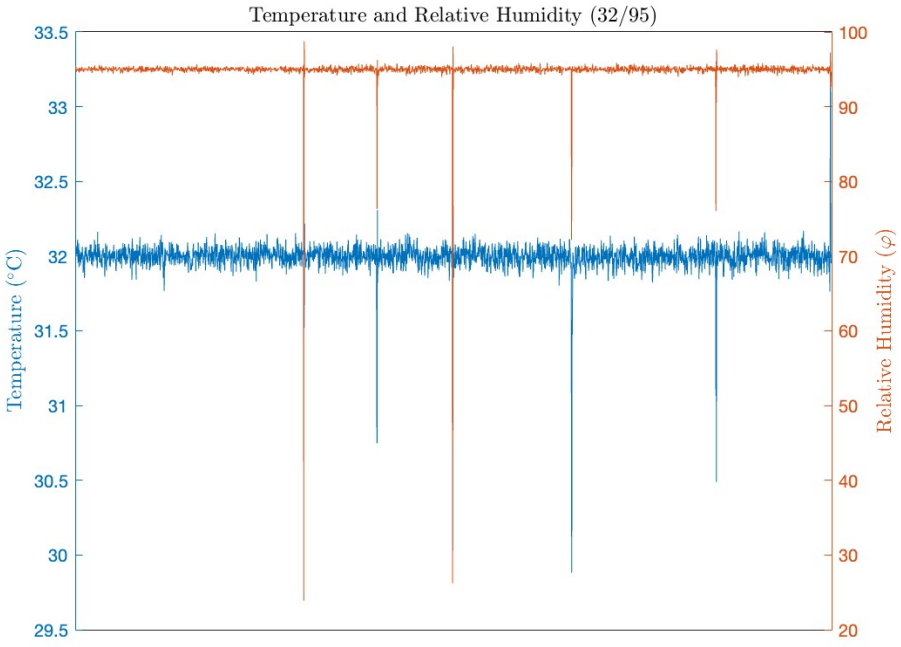

Figure A.4: Temperature = 32 °C, $\varphi = 95$

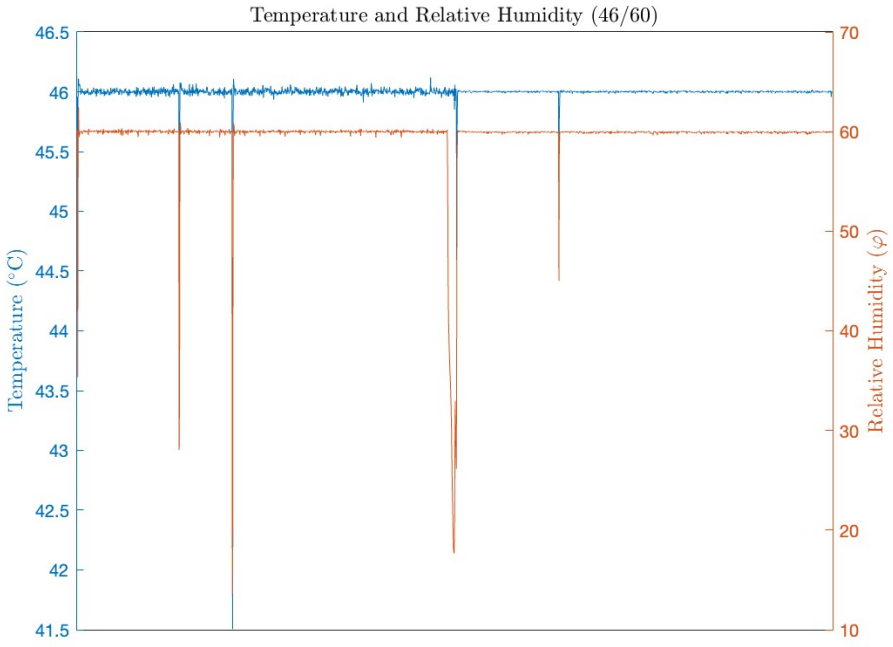

Figure A.5: Temperature = 46 °C, $\varphi = 60$

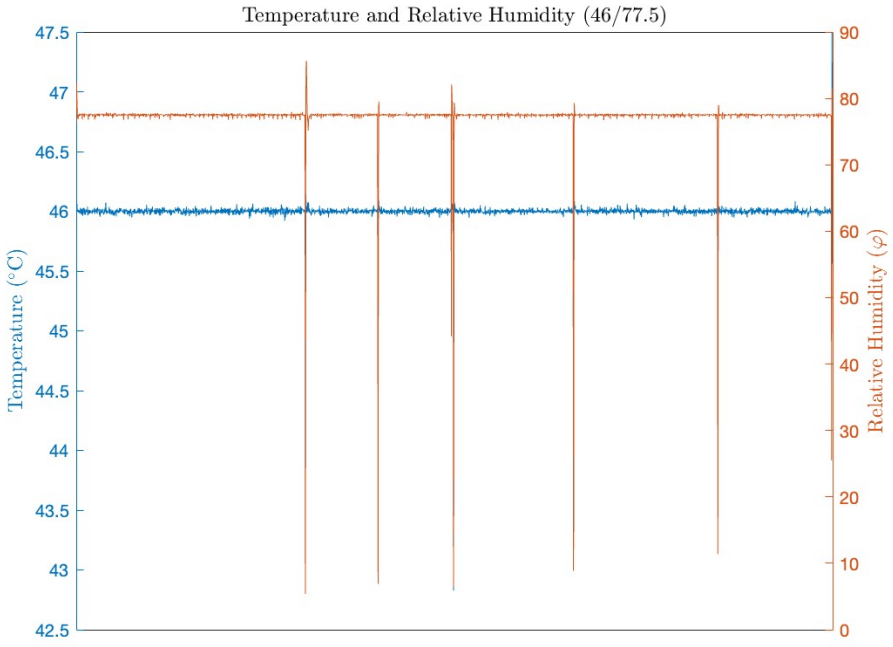

Figure A.6: Temperature = 46 °C, $\varphi = 77.5$

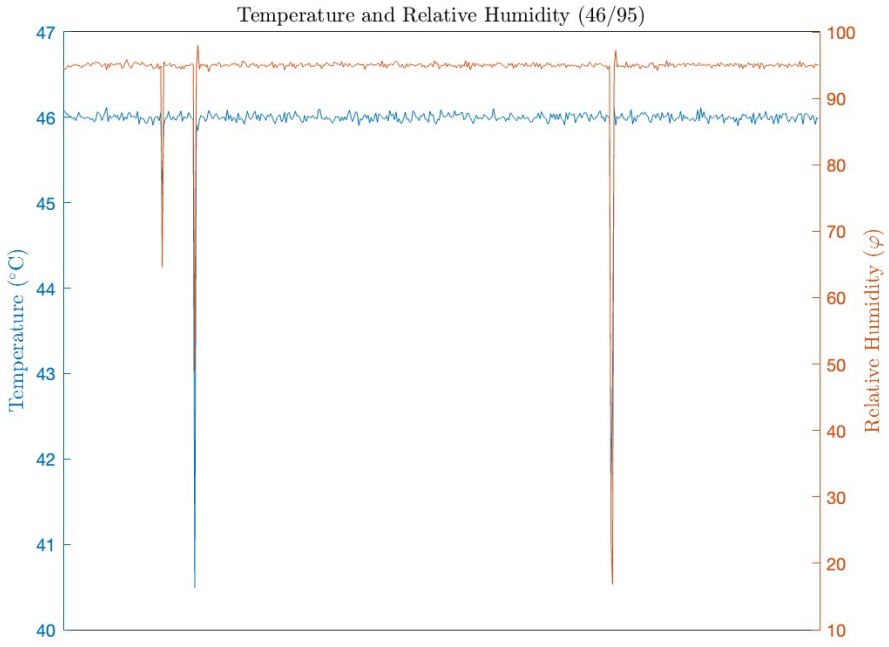

Figure A.7: Temperature = 46 °C, $\varphi = 95$

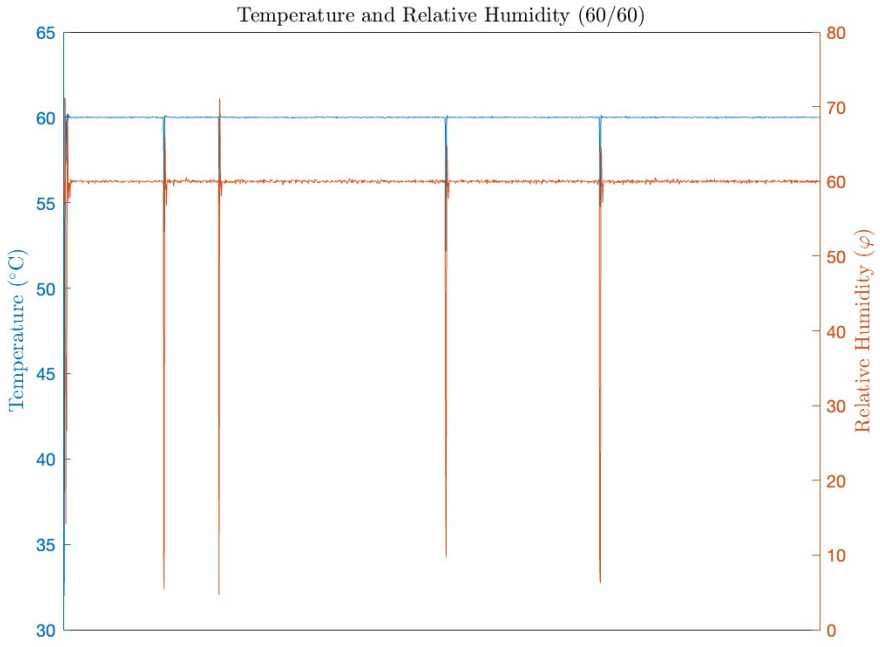

Figure A.8: Temperature = 60 °C, $\varphi = 60$

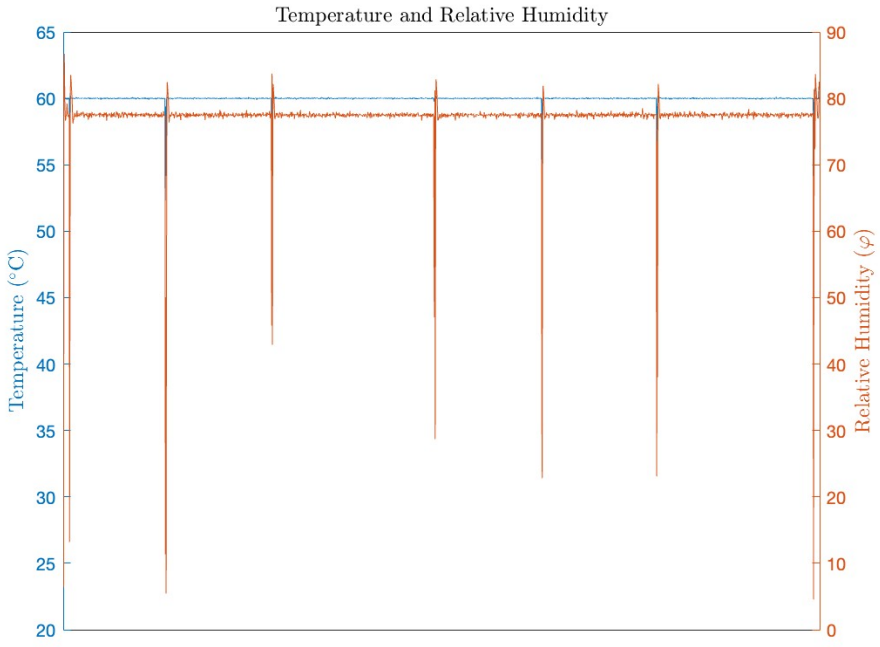

Figure A.9: Temperature = 60 °C, $\varphi = 77.5$

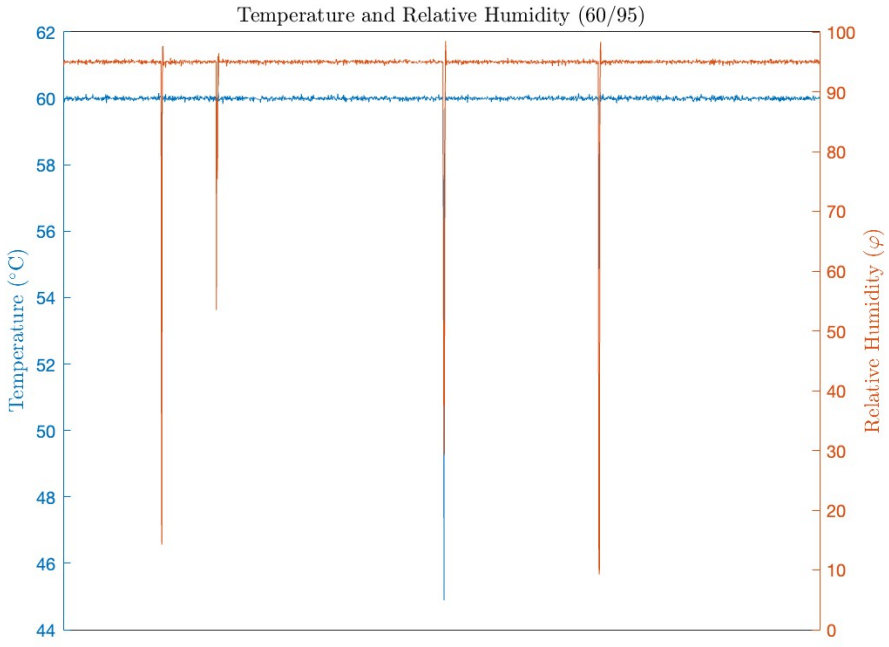

Figure A.10: Temperature = 60 °C, $\varphi = 95$

Appendix B

Work Distribution

Table B.1: Work distribution

Task	Philip	Erik
Literature review	50%	50%
Map current test methods	50%	50%
Stakeholder input	50%	50%
Evaluation of current standard	50%	50%
Data collection	50%	50%
Data Analysis	50%	50%
Testing samples	50%	50%

Appendix C

Gantt chart

				Jan			Feb				Mar				Apr					May				Jun
Task	Begin	End	Days	W. 3	W. 4	W. 5	W. 6	W. 7	W. 8	W. 9	W. 10	W. 11	W. 12	W. 13	W. 14	W. 15	W. 16	W. 17	W. 18	W. 19	W. 20	W. 21	W. 22	W. 23
Litterature review	2024-01-15	2024-02-05	22	x	x	x	x																	
Data collection	2024-01-15	2024-02-05	22	x	x	x	x																	
Interviews	2024-01-29	2024-02-12	15			x	x	x																
Data Anslysis	2024-02-12	2024-02-26	15					x	x	x														
Map current test methods	2024-02-05	2024-03-04	29				x	x	x	x	x													
Industry test method	2024-02-12	2024-03-04	22					x	x	x	x													
Stakeholder input	2024-02-26	2024-03-11	15							x	x	x												
Testing samples	2024-02-05	2024-04-01	57				x	x	x	x	x	x	x	x	x									
Evaluation of current standard	2024-03-11	2024-03-25	15									x	x	x										
Requirments	2024-03-25	2024-05-06	43											x	x	x	x	x	x	x				
Product specification	2024-03-25	2024-05-06	43											x	x	x	x	x	x	x				
New test methods	2024-03-25	2024-05-06	43											x	x	x	x	x	x	x				
Thesis report	2024-01-15	2024-05-27	134	x	x	x	x	x	x	x	x	x	x	x	x	x	x	x	x	x	x	x	x	
Opposition	2024-06-03	2024-06-03	1																					x

Figure C.1: Original time plan

				Jan			Feb				Mar				Apr					May			
Task	**Begin**	**End**	**Days**	W. 3	W. 4	W. 5	W. 6	W. 7	W. 8	W. 9	W. 10	W. 11	W. 12	W. 13	W. 14	W. 15	W. 16	W. 17	W. 18	W. 19	W. 20	W. 21	W. 22
Litterature review	2024-01-15	2024-04-08	85	x	x	x	x	x	x	x					x	x							
Map current test methods	2024-01-15	2024-02-05	22	x	x	x	x																
Stakeholder input	2024-01-15	2024-02-05	22	x	x	x	x																
Evaluation of current standard	2024-01-15	2024-02-05	22	x	x	x	x																
Thesis report	2024-01-15	2024-05-20	127	x	x	x	x	x	x	x	x	x	x	x	x	x	x	x	x	x	x	x	
Data collection	2024-01-29	2024-02-05	8			x	x																
Data Analysis	2024-02-12	2024-05-20	99					x	x	x										x	x	x	
Testing samples	2024-03-04	2024-05-06	64								x	x	x	x	x	x	x	x	x	x			
Opposition	2024-05-27	2024-05-27	1																				x

Figure C.2: Actual time plan